Heliyon 10 (2024) e37819

Contents lists available at ScienceDirect

Heliyon

journal homepage: www.cell.com/heliyon

Research article

An enhanced snow ablation optimizer for UAV swarm path planning and engineering design problems

Jinyi Xie [a], Jiacheng He [b], Zehua Gao [c], Shiya Wang [d], Jingrui Liu [e], Hanwen Fan [f,*]

[a] School of Mathematics and Information Science, Guangzhou University, Guangzhou, 510000 China
[b] School of Economics and Management, China University of Mining and Technology, Xuzhou, 221116, China
[c] International College, Hebei University, Baoding, 071002, China
[d] School of Chemical Engineering, East China University of Science and Technology, Shanghai, 200237, China
[e] Chongqing University–University of Cincinnati Joint Co-op Institute, Chongqing, 400044, China
[f] School of Computer Science and Technology, Dalian University of Technology, Dalian, 116024, China

ARTICLE INFO

Keywords:
Snow ablation optimizer
Metaheuristic algorithm
Numerical optimization
UAV swarm path planning
Engineering design problems

ABSTRACT

The Snow Ablation Optimizer (SAO) is an advanced optimization algorithm. However, it suffers from slow convergence and a tendency to become trapped in local optima. To address these limitations, we propose an Enhanced Snow Ablation Optimization algorithm (ESAO). Initially, an adaptive T-distribution control strategy is employed to improve the algorithm's exploratory position adjustments, facilitating the identification of the global optimum. Furthermore, we introduce a Cauchy mutation strategy, endowing individuals with a robust capability to escape local extrema and steer the population towards more favorable directions. A leader-based boundary control strategy is also proposed to enhance the optimizer's search performance, significantly increasing the accuracy, speed, and stability of the algorithm in tackling complex problems. To validate the performance of ESAO, we utilize 29 CEC2017 benchmark functions for comparison against eight popular algorithms across various dimensions. Our algorithm ranked first in all comparisons, demonstrating ESAO's effectiveness. Additionally, to evaluate the practical applicability of the proposed method, we mathematically modeled the UAV swarm and solved the UAV swarm path planning problem using various competitor algorithms. Furthermore, we applied different competitor algorithms to two engineering design problems. The results demonstrate that ESAO performs the best. In general, ESAO outperforms its counterparts in terms of solution quality and stability, showcasing its superior application potential.

1. Introduction

UAV swarms are emerging with new applications to address the challenges of industrial and emergency scenarios. Their low cost, high mobility, enhanced security, and portable size are the key factors contributing to their wide application [1,2]. Diverse UAVs can be equipped with sensors of various functions to adapt to different mission requirements. Particularly in the field of remote sensing, sensor technology utilized by UAVs is rapidly advancing, and their flexibility and customizability make them an ideal choice for addressing a wide range of problems [3]. Traditional methods are inefficient in solving UAV swarm path planning. Metaheuristic algorithms have garnered significant attention in the field of UAV swarm path planning due to their efficiency and adaptability [4].

* Corresponding author.
E-mail address: hanwen_fan@163.com (H. Fan).

https://doi.org/10.1016/j.heliyon.2024.e37819
Received 26 May 2024; Received in revised form 28 July 2024; Accepted 10 September 2024
Available online 11 September 2024

Metaheuristics are classified into four categories based on their source of inspiration [5]: physical heuristics, swarm intelligence, evolutionary algorithms, and human behavior heuristics. Among these, physical heuristics draw inspiration from physical laws and mathematical theories. For instance, the simulated annealing algorithm, developed by Kirkpatrick et al. [6], is based on the process of substances achieving thermal equilibrium. Swarm intelligence algorithms are designed to mimic the collective behavior of social creatures [7]. For instance, Mirjalili et al. [8] introduced the Grey Wolf optimizer, inspired by the hunting behavior of grey wolves. Evolutionary algorithms replicate the selection and genetic mechanisms found in nature [9], for instance, the genetic algorithm introduced by Holland [10], which is inspired by Darwin's theory of natural selection. Lastly, human behavior heuristics, like the Social Evolution and Learning Optimization Algorithm (SELOA) developed by Kumar et al. [11], are modeled after human social learning patterns.

In general, the metaheuristic algorithm search process usually consists of two phases: exploration and exploitation [12]. In the exploration phase, the algorithm comprehensively explores the search space to find diverse solutions for a given problem. In contrast, during the exploitation phase, the algorithm uses local information to generate better solutions, often close to the current solution. It is crucial for metaheuristics to balance these two phases, as over-exploration slows down convergence, while over-exploitation may lead to getting stuck in local optima [13]. The key to global optimization, engineering problems, and UAV swarm path planning is balancing the two phases of exploration and exploitation. Metaheuristic algorithms are widely used to solve such problems, as they can find near-global optimal solutions in a limited time. However, it is important to note that, due to the No Free Lunch theorem (NFL) [14], the uniqueness of different problems necessitates the development of specialized algorithms for specific challenges to guarantee optimal and efficient solutions.

The Snow Ablation Optimizer (SAO) is a physics-based optimization technique proposed by Deng et al. [15] in 2023. This paper primarily simulates the physical phenomena of snow sublimating into water vapor and melting into liquid water, as well as the transformation of liquid water into water vapor. Simultaneously, a dual-population mechanism is introduced to achieve a balance between the exploitation and exploration phases of the optimizer. However, the Snow Ablation Optimization algorithm occasionally encounters issues such as slow convergence, a tendency to fall into local optima, and suboptimal practical application results. To overcome these limitations, this paper introduces an Enhanced Snow Ablation Optimizer (ESAO).

1) An update rule based on adaptive t-distribution is proposed to reduce the risk of falling into local optima.
2) **Introducing the Cauchy mutation selection mechanism** aims to ensure accuracy and to improve the convergence speed.
3) A control strategy based on the leader's boundaries is put forward, leading individuals to move and effectively utilizing the information of the entire population to find the optimal solution.
4) The widely used CEC2017 test set is employed, with three different dimensions to verify ESAO's global optimization ability.
5) ESAO can be applied to UAV swarm path planning and two engineering design problems, further verifying its effectiveness and robustness in solving practical problems.

The rest of this article is organized as follows: Section II reviews the original SAO. Section III elaborates the proposed ESAO. In Section IV, numerical experiments and analysis are carried out. Section V describes the real-world applications model and simulation analysis. Conclusions are reported in Section VI.

2. Related work

In this section, we will introduce some popular metaheuristic algorithms in recent years and some algorithms with applications in UAV swarm path planning.

In 2022, Ayyarao et al. [16] proposed a metaheuristic optimization algorithm based on ancient war strategies. The proposed War Strategy Optimization (WSO) algorithm is inspired by the strategic movement of troops during a war. Inspired by the cooperative hunting behavior of the golden jackal, Chopra et al. [17] proposed a new nature-inspired optimization method named the Golden Jackal Optimization (GJO) algorithm. Xue et al. [18] introduced a novel population-based technique called the Dung Beetle Optimizer (DBO) algorithm, which is inspired by the ball rolling, dancing, foraging, stealing, and breeding behaviors of dung beetles. Hashim et al. [19] introduced a novel natural heuristic metaheuristic called the Snake Optimizer (SO) to handle a series of optimization tasks, mimicking the special mating behavior of snakes.

In 2023, Shehadeh [20] developed the Chernobyl Disaster Optimizer (CDO), inspired by the core explosion of the Chernobyl nuclear reactor. Guan et al. [21] proposed the Great Wall Construction Algorithm (GWCA), which simulates the competition and elimination mechanism among workers during the construction of the Great Wall. The Optical Microscope Algorithm (OMA) draws inspiration from the amplification ability of the optical microscope for targeting objects [22]. Su et al. [23] developed a Frost Ice Optimizer to emulate the physical phenomenon of frost formation. The Subtraction-Average-Based Optimizer (SABO) was inspired by the concept of the subtraction mean [24]. Safavi et al. [25] developed a Geometric Mean Optimizer (GMO) that simulates the properties of geometric mean operators in mathematics. This optimizer can simultaneously evaluate the fitness and diversity of individuals in the search space. Kamran et al. [26] developed a Gold Rush Optimizer based on three key concepts of gold exploration. The Waterwheel Plant Algorithm (WWPA) was introduced to simulate the hunting and exploration behavior of waterwheel plants [27].

In 2024, Fang et al. [28] introduced a novel metaheuristic, the Wind-fallen Leaf Optimization (WLO), inspired by the natural phenomenon of wind-fallen leaves. Zhang et al. [29] proposed a new metaheuristic optimization algorithm called the Clean Fish Optimization (CFO) Algorithm, inspired by clean fish behavior. Sowmya et al. [30] developed a new metaheuristic algorithm, the Newton-Raphson-Based Optimizer (NRBO), inspired by the Newton-Raphson method, which explores the search process using two rules. Fu et al. [31] proposed a novel metaheuristic called the Red-beak Blue Magpie Optimizer (RBMO), inspired by the cooperative and efficient predation behavior of red-beak blue magpies, for 2D/3D UAV path planning. Tian et al. [32] proposed a novel nature-inspired metaheuristic called the Snow Geese Algorithm (SGA), inspired by the migratory behavior of snow geese and mimicking the unique “herringbone” and “straight line” flight patterns observed during their migration. Wang et al. [33] innovatively proposed the Black Kite Algorithm (BKA), a metaheuristic optimization algorithm inspired by the migration and predation behavior of black kites. Fu et al. [34] introduced a population-based metaheuristic algorithm called the Secretary Bird Optimization Algorithm (SBOA), inspired by the survival behavior of secretary birds in natural environments, for 3D UAV path planning.

Many algorithms have been applied to UAV swarm path planning. For example, He et al. [35] demonstrated a multi-UAV cooperative path planning approach based on a hybrid particle swarm optimization algorithm. Lu et al. [36] incorporated an uncertain search mechanism and bidirectional planning method into the traditional artificial bee colony algorithm. They enhanced the food generation method within the artificial bee colony algorithm and proposed an improved RB-ABC algorithm, which was successfully applied to UAV swarm path planning. Li et al. [37] addressed the path planning problem for multiple UAVs under various wind field conditions and proposed an Improved Honey Badger Algorithm-Fruit Fly Optimization Algorithm (HBAFOA) to solve it.These studies demonstrate the effectiveness of metaheuristic algorithms in UAV path planning. As a new high-performance algorithm, SAO has been improved by researchers and applied to many real-world fields [38,39], but it has not yet been used to solve the path planning problem of UAV swarms. Therefore, addressing the issues of SAO in global optimization and engineering problems, and its lack of application in UAV group path planning, this paper proposes an enhanced SAO technology.

3. The proposed methodology

In this section, we describe the original SAO and the proposed ESAO in detail.

3.1. Snow ablation optimizer (SAO)

This section describes the inspiration and mathematical model of SAO.

3.1.1. Inspiration source of SAO

Snow is among the most beautiful phenomena in nature, especially during winter. Snowmelt plays a crucial role in ecosystems, influencing the growth of crops and impacting human health [40]. From a physical perspective, snow can transform into liquid water and water vapor. This involves two primary physical processes: melting and sublimation. Snow melts, transforming into liquid water, whereas sublimation converts snow directly into water vapor. Furthermore, melted water can further evaporate into steam. The Snow Ablation Optimizer (SAO) draws inspiration from the sublimation and melting processes of snow in natural environments.

3.1.2. Population initialization

The iterative process of SAO starts with randomly generated populations. It is represented as a $N \times \text{Dim}$ matrix, as shown in Eq. (1).

$$Z=\begin{bmatrix} z_{1,1} & z_{1,2} & \cdots & z_{1,Dim-1} & z_{1,Dim} \\ z_{2,1} & z_{2,2} & \cdots & z_{2,Dim-1} & z_{2,Dim} \\ \vdots & \vdots & \vdots & \vdots & \vdots \\ z_{N-1,1} & z_{N-1,2} & \cdots & z_{N-1,Dim-1} & z_{N-1,Dim} \\ z_{N,1} & z_{N,2} & \cdots & z_{N,Dim-1} & z_{N,Dim} \end{bmatrix}_{N\times Dim} \tag{1}$$

where N represents the population size and Dim denotes the dimensional size.

3.1.3. Exploration phase

The exploration strategy constitutes the core of SAO. This irregular motion, occurring as snow or liquid water converts to steam, results in a high dispersion of the search agent. This phenomenon is represented through Brownian motion, a stochastic process widely utilized to model animal foraging, particle movement, and stock price fluctuations, among other applications. The step size of standard Brownian motion is governed by a normal distribution, with a mean of 0 and a variance of 1, as given in Eq. (2) [41]:

$$RB(Dim) = \frac{1}{\sqrt{2\pi}}\exp\left(-\frac{x^2}{2}\right) \tag{2}$$

Through dynamic and uniform step size, Brownian motion explores the potential area in the search space, simulating the diffusion of steam in the search space. Therefore, the location update formula during the exploration process is given by Eq. (3).

$$Z_i(t+1) = Elite(t) + RB(Dim) \times (\theta_1 \times (G(t) - Z_i(t)) + (1-\theta_1) \times (\overline{Z}(t) - Z_i(t))) \tag{3}$$

where $Z_i(t)$ represents the ith agent in the tth iteration, $RB(Dim)$ denotes the Brownian motion, and θ_1 is the number chosen at random from [0,1]. In addition, $G(t)$ refers to the current best solution, $Elite(t)$ is an individual chosen at random from the elite of the group, and $\overline{Z}(t)$ presents the position of the center of mass of the entire group. The corresponding mathematical expression is denoted in Eq. (4)

$$\overline{Z}(t) = \frac{1}{N}\sum_{i=1}^{N} Z_i(t) \tag{4}$$

$$Elite(t) \in [G(t), Z_{second}(t), Z_{third}(t), Z_c(t)] \tag{5}$$

where $Z_{second}(t)$ and $Z_{third}(t)$ are the second and third of the current population individuals, respectively. $Z_c(t)$ denotes the top 50 % of individual fitness value (leader) centroid position, calculating by using Eq. (6).

$$Z_c(t) = \frac{1}{N_1}\sum_{i=1}^{N_1} Z_i(t) \tag{6}$$

where N_1 denotes the number of leaders, that is, half the size of the group. $Z_i(t)$ shows the ith best leader. In each iteration, $Elite(t)$ demonstrates randomly selected from a set containing the current best solution, the second and third best individuals, and the leader 's centroid position.

3.1.4. Exploitation phase

In the SAO algorithm, the exploitation features are emphasized. When the snow melts into water, the search agent is encouraged to concentrate on exploiting high-quality solutions around the current optimum. The mathematical model is reported in Eq. (7).

$$Z_i(t+1) = M \times G(t) + RB(Dim) \times (\theta_2 \times (G(t) - Z_i(t)) + (1-\theta_2) \times (\overline{Z}(t) - Z_i(t))) \tag{7}$$

where M denotes the snowmelt rate, and the mathematical model is denoted in Eq. (8), θ_2 represents a number randomly selected from the [-1,1] interval to enhance the interaction between individuals. In this process, with the help of the two cross terms $\theta_2\times(G(t) - Z_i(t))$ and $(1-\theta_2)\times(\overline{Z}(t) - Z_i(t))$, individuals are more inclined to use the current optimal solution and group center information to develop potentially valuable regions.

$$M = \left(0.35 + 0.25 \times \frac{e^{\frac{t}{t_{max}}} - 1}{e-1}\right) \times T(t), T(t) = e^{\frac{-t}{t_{max}}} \tag{8}$$

where $T(t)$ represents the current temperature [42], t_{max} is the maximum number of iterations, t denotes the current number of iterations.

3.1.5. Two-population mechanism

A dual group mechanism [43,44] is devised to simulate the transformation process from snow to water to steam, representing the exploration and exploitation behavior of individuals in the solution space. In the initial stage, the algorithm randomly divides all individuals into two equally sized subgroups, each responsible for exploration and exploitation, respectively. As the iteration progresses, the size of the exploration group gradually increases, while the size of the exploitation group decreases correspondingly, to adapt and simulate the shift in individual behavior from centralized exploitation to extensive exploration. Pseudocode for this procedure is reported as **Algorithm 1**.

Algorithm 1 Pseudocode of Dual-population mechanism.

```
Begin
Initialize related parameters: Na = Nb = N/2, where Na represents the number of explored individuals, Nb denotes the number of exploited individuals
While t < tmax+1
      If Na < N
         Na = Na+1, Nb = Nb-1
      End if
End while
End
```

To summarize, the pseudocode of the SAO algorithm is shown in **Algorithm 2**.

Algorithm 2 Pseudocode of SAO Algorithm.

```
Begin
Initialize related parameters
     Using Eq. (1) Initialize the population
While t < tmax+1
      Calculate M by using Eq. (8)
      for each agent
         Exploration phase: Updating individual position by Eq. (3)
         Updating sub-population by Algorithm 1
```

(continued on next page)

(*continued*)

Algorithm 2 Pseudocode of SAO Algorithm.
Exploitation phase: *Updating individual position by Eq. (7)*
end for
Fitness evaluation
Updating G(t)
$t = t+1$
end while
End

3.2. *The proposed ESAO*

In this section, the ESAO algorithm is proposed, and we design three improvement strategies to solve the problem of SAO low accuracy and easy to fall into local optimum.

3.2.1. *Motivation*

These strategies were chosen for this work for the following reasons.

1) An update rule based on adaptive t-distribution is proposed to reduce the risk of falling into local optima. The traditional SAO algorithm may be constrained by fixed distribution shapes, making it prone to getting stuck in local optima, especially in complex search spaces. The adoption of an adaptive t-distribution allows for adjusting the shape of the distribution according to the current search state, making it more adaptable to the characteristics of the search space. This increases the likelihood of escaping local optima and enhances the algorithm's capability for global exploration.
2) The introduction of the Cauchy mutation selection mechanism aims to ensure accuracy and to improve convergence speed. The Cauchy distribution, with its heavy-tailed nature, is better suited for exploring distant regions in the search space. By incorporating the Cauchy mutation selection mechanism, the algorithm can explore various corners of the search space more effectively, thus increasing both the breadth and depth of the search. This accelerates convergence speed and enables the algorithm to potentially find superior solutions in shorter time frames.
3) A control strategy based on the leader's boundaries is proposed, guiding individuals to move, and effectively utilizing the information of the entire population to find the optimal solution. Leaders play a crucial role in optimization algorithms, as their positions and states directly influence the behavior of the entire population. By introducing a control strategy based on the leader's boundaries, we ensure that individuals do not deviate from the target region during the search process. Additionally, leveraging the information from leaders guides the entire population towards the direction of the global optimum, thereby enhancing the convergence and search efficiency of the algorithm.

3.2.2. *Adaptive T-distribution control strategy (SAO1)*

The T-distribution, also known as the Student's distribution [45], was first introduced by the British statistician William Sealy Gosset [46]. The optimizer requires position changes during the exploration process to locate the global optimal solution more effectively. Thus, a distribution strategy is employed to update the position of snowmelt particles. The mathematical model is presented in Eq. (9).

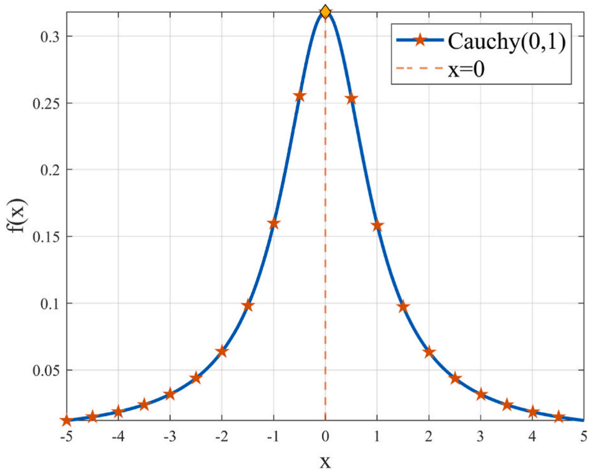

Fig. 1. Standard Cauchy distribution probability density.

$$Z_i(t+1) = Elite(t) + trnd(Dof) \times RB(Dim) \times (\theta_1 \times (G(t) - Z_i(t)) + (1-\theta_1) \times (\overline{Z}(t) - Z_i(t))) \tag{9}$$

where $trnd(Dof)$ represents the adaptive t-distribution, and Dof is the degree of freedom, as shown in Eq. (10).

$$Dof = \omega_1 + \frac{\omega_2 \times t}{t_{max}} \tag{10}$$

3.2.3. Selection mechanism of cauchy mutation (SAO2)

In order to better reflect the law of continuous replacement and transformation in the exploitation process of snow melting optimizer, we introduce Cauchy mutation strategy. Cauchy mutation is derived from the Cauchy distribution [47], and its one-dimensional probability density function is denoted in Eq. (11).

$$f(x) = \left(\frac{1}{\pi}\right) \times \left(\frac{a}{a+x^2}\right), x \in (-\infty, +\infty) \tag{11}$$

When $a = 1$, the distribution is termed the standard Cauchy distribution. As observed in Fig. 1, the Cauchy distribution is characterized by a long and flat tail at both ends, with a relatively smooth approach towards 0. This characteristic allows the Cauchy distribution to generate random numbers distant from the mean, enhancing the ability of individuals to escape local extrema following a Cauchy mutation. Consequently, we introduce the search method described by Eq. (12).

$$Z_i(t+1) = M \times G(t) + cauchy \times RB(Dim) \times (\theta_2 \times (G(t) - Z_i(t)) + (1-\theta_2) \times (\overline{Z}(t) - Z_i(t))) \tag{12}$$

The $cauchy$ denotes Cauchy mutation operator, as shown in Eq. (13).

$$cauchy = 1 + \tan(0.5 \times \pi \times (rand - 0.5)) \tag{13}$$

The $rand$ represents a random number from 0 to 1.

3.2.4. Leader-based boundary control strategy (SAO3)

The traditional boundary control strategy fails to enhance the search performance of the algorithm [23]. Therefore, we introduce a leader-based boundary control strategy aimed at enhancing the search performance of the optimizer. The improvements are as follows: First, under the guidance of the leader, both the objective and speed of the search are enhanced, thereby enabling the algorithm to identify the optimal solution more rapidly. Second, by precisely setting the search boundaries, invalid searches are minimized, and computational efficiency is enhanced. Third, adjusting the position and search range of the leader enhances the algorithm's adaptability to various complex scenarios. Fourth, maintaining solution diversity prevents the algorithm from prematurely converging to local optima. In summary, this strategy significantly enhances the accuracy, speed, and stability of the algorithm in addressing complex problems. The mathematical model is presented in Eq. (14) and Eq. (15).

$$Z_i(t+1) = (G(t) + Ub) \div 2 \tag{14}$$

$$Z_i(t+1) = (G(t) + Lb) \div 2 \tag{15}$$

where Ub and Lb represent the upper and lower bounds of the search problem, respectively.

In summary, the pseudocode of the ESAO algorithm is denoted in **Algorithm 3**.

Algorithm 3 Pseudocode of ESAO Algorithm.

```
Begin
Initialize related parameters
    Using Eq. (1) Initialize the population
While t < t_max+1
        Calculate M by using Eq. (8)
        For each agent
            Exploration phase: Updating individual position by Eq. (9)
            Updating sub-population by Algorithm 1
            Exploitation phase: Updating individual position by Eq. (12)
    The boundary is adjusted by Eq. (14) and Eq. (15)
        End for
        Fitness evaluation
        Updating G(t)
        t = t+1
End while
End
```

3.2.5. Time complexity analysis

This section analyzes the time complexity of the SAO and ESAO algorithms. Suppose, the number of solutions is N, t_{max} denotes the maximum number of iterations, Dim represents the dimension size of the solved problem. The complexity of population initialization and location update is $O(N \times Dim)$, the complexity of fitness evaluation is $O(N)$, and the complexity of fitness ranking is $O(N \times log(N))$. The complexity of the main calculation mainly involves the number of fitness evaluations. In this paper, the three strategies we propose change the update rules of the original algorithm and do not increase the fitness calculations, that is, they do not increase the original complexity of the algorithm. Therefore, the total time complexity is estimated as $O(ESAO) = O(SAO) = O(N \times Dim + N \times t_{max} \times (log(N) + Dim + 1))$.

4. Numerical experiments

In this section, we present a numerical analysis of ESAO and other competitor algorithms.

4.1. Review the CEC2017 test suite

This section utilizes the CEC2017 (Dimensions = 30, 50, 100) test suite to evaluate the performance of the proposed ESAO algorithm [48]. The suite comprises four types of functions: unimodal, multimodal, mixed, and composite. The unimodal function, possessing a single optimal solution, evaluates the algorithm's convergence speed and exploitation ability. The other three types of functions, featuring multiple optimal solutions, assess the algorithm's ability to avoid local optima and its global exploration capability. Refer to Table 1 for a detailed description of the suite.

4.2. Algorithm parameter settings

ESAO is compared with eight other popular meta-heuristic algorithms, encompassing classic, state-of-the-art, and high-performance variants: WOA [49], SSA [50], GJO [17], COA [51], PPSO [52], DECMSA [53], MELGWO [54], and SAO [15]. Comparison parameters for these algorithms are detailed in Table 2. Each algorithm was configured with a maximum of 500 iterations, a population size of 50, and was run independently 30 times to record the experiment's results. Ultimately, the data were processed to calculate the average value (Avg) and standard deviation (Std), with the best results highlighted in bold.

Table 1
CEC2017 detailed introduction.

Type	ID	Description	Dim	$f_{\min}$
Unimodal	CEC2017-F1	Shifted and Rotated Bent Cigar Function	30/50/100	100
	CEC2017-F3	Shifted and Rotated Zakharov Function	30/50/100	300
Multimodal	CEC2017-F4	Shifted and Rotated Rosenbrock's Function	30/50/100	400
	CEC2017-F5	Shifted and Rotated Rastrigin's Function	30/50/100	500
	CEC2017-F6	Shifted and Rotated Expanded Scaffer's F6 Function	30/50/100	600
	CEC2017-F7	Shifted and Rotated Lunacek Bi_Rastrigin Function	30/50/100	700
	CEC2017-F8	Shifted and Rotated Non-Continuous Rastrigin's Function	30/50/100	800
	CEC2017-F9	Shifted and Rotated Levy Function	30/50/100	900
	CEC2017-F10	Shifted and Rotated Schwefel's Function	30/50/100	1000
Hybrid	CEC2017-F11	Hybrid Function 1 (N = 3)	30/50/100	1100
	CEC2017-F12	Hybrid Function 2 (N = 3)	30/50/100	1200
	CEC2017-F13	Hybrid Function 3 (N = 3)	30/50/100	1300
	CEC2017-F14	Hybrid Function 4 (N = 4)	30/50/100	1400
	CEC2017-F15	Hybrid Function 5 (N = 4)	30/50/100	1500
	CEC2017-F16	Hybrid Function 6 (N = 4)	30/50/100	1600
	CEC2017-F17	Hybrid Function 6 (N = 5)	30/50/100	1700
	CEC2017-F18	Hybrid Function 6 (N = 5)	30/50/100	1800
	CEC2017-F19	Hybrid Function 6 (N = 5)	30/50/100	1900
	CEC2017-F20	Hybrid Function 6 (N = 6)	30/50/100	2000
Composition	CEC2017-F21	Composition Function 1 (N = 5)	30/50/100	2100
	CEC2017-F22	Composition Function 2 (N = 5)	30/50/100	2200
	CEC2017-F23	Composition Function 3 (N = 5)	30/50/100	2300
	CEC2017-F24	Composition Function 4 (N = 5)	30/50/100	2400
	CEC2017-F25	Composition Function 5 (N = 3)	30/50/100	2500
	CEC2017-F26	Composition Function 6 (N = 3)	30/50/100	2600
	CEC2017-F27	Composition Function 7 (N = 5)	30/50/100	2700
	CEC2017-F28	Composition Function 8 (N = 5)	30/50/100	2800
	CEC2017-F29	Composition Function 9 (N = 5)	30/50/100	2900
	CEC2017-F30	Composition Function 10 (N = 3)	30/50/100	3000
Search Range: [-100,100]				

Table 2
Parameter Settings for the selected competitor algorithm.

Algorithm	Name of the parameter	Value of the parameter
WOA	a, a2, b	[0,2], [-1,-2], 1
SSA	C1	[0,2]
GJO	E1, E0	[0,1.5], [-1,1],
COA	C, T	[0,2] [20,35],
PPSO	θ	$[0, 2\pi]$
DECMSA	p, c	0.5, 0.1
MELGWO	pCR, Fmin, Fmax, a	0.6, 0.1, 2, [0,2]
SAO	T, DDF	[1/e, 1], [0.35, 0.6]
ESAO	T, DDF, ω_1, ω_2	[1/e, 1], [0.35, 0.6], 4, 3

4.3. Ablation experiment

In this section, we conduct an impact analysis on the proposed ESAO, SAO, and their associated improvement strategies (SAO1, SAO2, and SAO3). The experimental results are presented in Fig. 2. It is evident from the results obtained with unimodal functions that these strategies have enhanced the original SAO algorithm. However, with multimodal functions, both individual improvement strategies and combinations of two strategies have demonstrated inferior performance. Only the ESAO algorithm, integrating all three improvement strategies, surpasses SAO in terms of global optimization. Therefore, the advancement of ESAO proves to be crucial.

4.4. Parameter sensitivity analysis

In this section, we perform a sensitivity analysis on the main parameters of ESAO, namely ω_1 and ω_2. We set a total of nine sets of parameters, as shown in Table 3. We then use the three dimensions of CEC2017 for simulation analysis, and the Friedman test results are reported in Table 4. From the results, it can be found that Case6 is the best and only slightly worse than Case5 when the dimension is 50. The last column shows the average ranking across all dimensions. Case6 ranks first with a Friedman value of 4.10, therefore, we set $\omega_1 = 4$ and $\omega_2 = 3$ in this article.

4.5. Convergence behavior analysis

To assess ESAO's performance, benchmark functions were utilized to analyze its convergence properties. As depicted in Fig. 3, the first column displays a 3D image of the benchmark function, intuitively revealing the complexity of the search space. The second column illustrates the search agent's trajectory, with most solution sets concentrated near the current optimal solution yet widely distributed, indicating ESAO's effective balance between exploration and exploitation. The third column details the average fitness value changes of the search agent, which are initially high, suggesting comprehensive exploration of the search space, and then rapidly

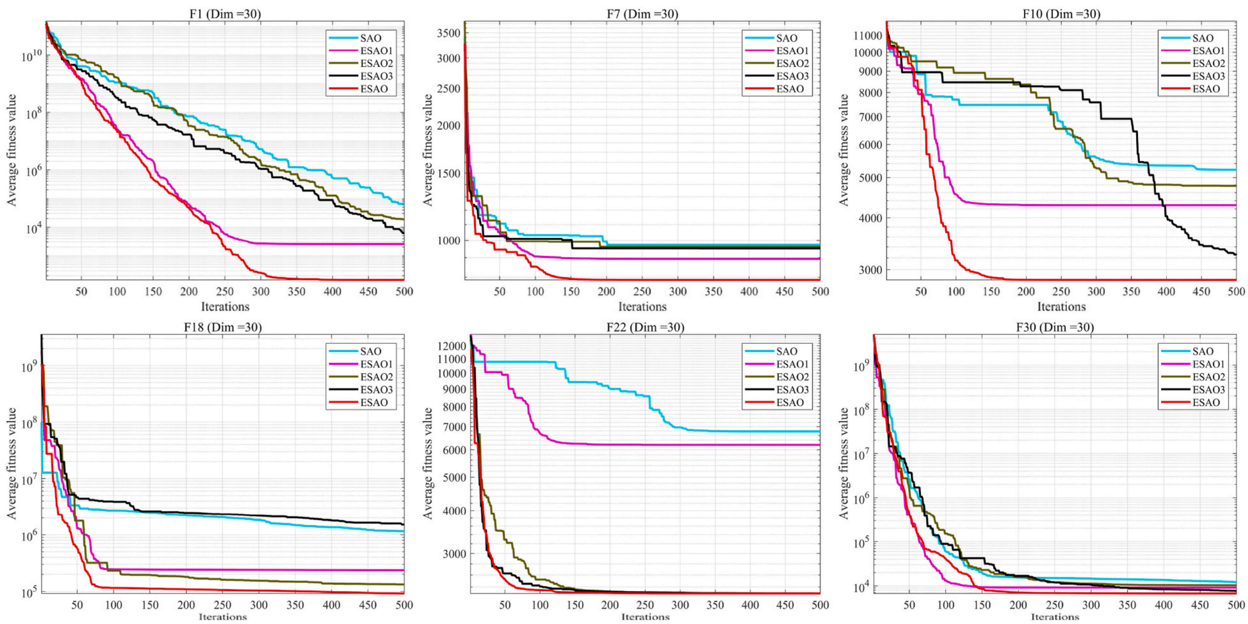

Fig. 2. Results of ablation experiment.

Table 3
Parameter settings.

Parameter	Case1	Case2	Case3	Case4	Case5	Case6	Case7	Case8	Case9
ω_1	2	2	2	4	4	4	6	6	6
ω_2	1	2	3	1	2	3	1	2	3

Table 4
Parameter sensitivity analysis results.

ID	Case1	Case2	Case3	Case4	Case5	Case6	Case7	Case8	Case9
Dim = 30	6.61	4.89	4.52	4.67	4.59	**4.49**	5.03	5.08	5.13
Ranking	9	5	2	4	3	**1**	6	7	8
Dim = 50	7.49	5.71	4.43	4.44	**4.25**	4.27	4.71	4.82	4.87
Ranking	9	8	3	4	**1**	2	5	6	7
Dim = 100	8.61	7.16	5.73	4.50	3.97	**3.53**	3.79	3.93	3.79
Ranking	9	8	7	6	5	**1**	2	4	3
All	7.57	5.92	4.89	4.54	4.27	**4.10**	4.51	4.61	4.60
Ranking	9	8	7	4	2	**1**	3	6	5

decrease, signifying that search agents are nearing the optimal position. The fourth column depicts the search agent's trajectory, transitioning from fluctuation to stability, symbolizing the shift from global exploration to local exploitation. The final column displays the algorithm's convergence curve. Across all functions, the curves decline rapidly, indicating efficient solution finding with fewer iterations. Based on ESAO's convergence properties, its performance is deemed excellent.

4.6. *Comparison with other competitors*

This section evaluates ESAO's performance using the CEC2017 suite and compares it with eight competitors. The experimental results are detailed in Table 5, Table 6, and Table 7. The best result among the nine competitors is highlighted in bold. Notably, our algorithm appears in bold most frequently, and as dimensions increase, ESAO's performance increasingly outshines that of its competitors. Fig. 4 illustrates the convergence curves of various competitors across different dimensions. To mitigate potential random fluctuations, the average iteration curve over 30 repeated runs is plotted. The experimental results indicate that the ESAO algorithm exhibits faster convergence and greater accuracy. Finally, to assess the algorithm's stability, a box plot is presented in Fig. 5, showing ESAO's superior results and smaller errors. Overall, ESAO demonstrates greater robustness than its eight competitors.

4.7. *Statistical analysis*

4.7.1. *Wilcoxon rank sum test*

This section utilizes the non-parametric Wilcoxon rank sum test [55] to compare ESAO with eight competitors, with results detailed in Table 8, Table 9, and Table 10. A p-value below 0.05 signifies a significant difference between ESAO and the competing algorithms. Algorithms without significant differences are highlighted in bold. Experimental results demonstrate that as dimension complexity increases, the differences between ESAO and competing algorithms become increasingly significant. Notably, there is only one instance where no difference is observed when the dimension reaches 100. Thus, based on previous analyses, ESAO exhibits distinct performance advantages over competing algorithms, showcasing superior comprehensive performance.

4.7.2. *Friedman test*

This section employs the nonparametric Friedman mean rank test [56] to rank the ESAO algorithm and its competitors' experimental results on the CEC2017 test set. Table 11 details the results, indicating that ESAO's average rankings—1.90, 1.50, and 1.13 across three dimensions—are all first. This demonstrates that the ESAO algorithm outperforms its competitors, exhibiting superior overall performance.

5. Real-world applications

In this section, we present a real-world comparison between ESAO and other competitors.

5.1. *UAV swarm path planning*

In this section, we model and experiment UAV swarm path planning.

5.1.1. *Problem description*

In this section, we describe the cost calculation method of a single UAV in detail, and the specific process is as follows: The first

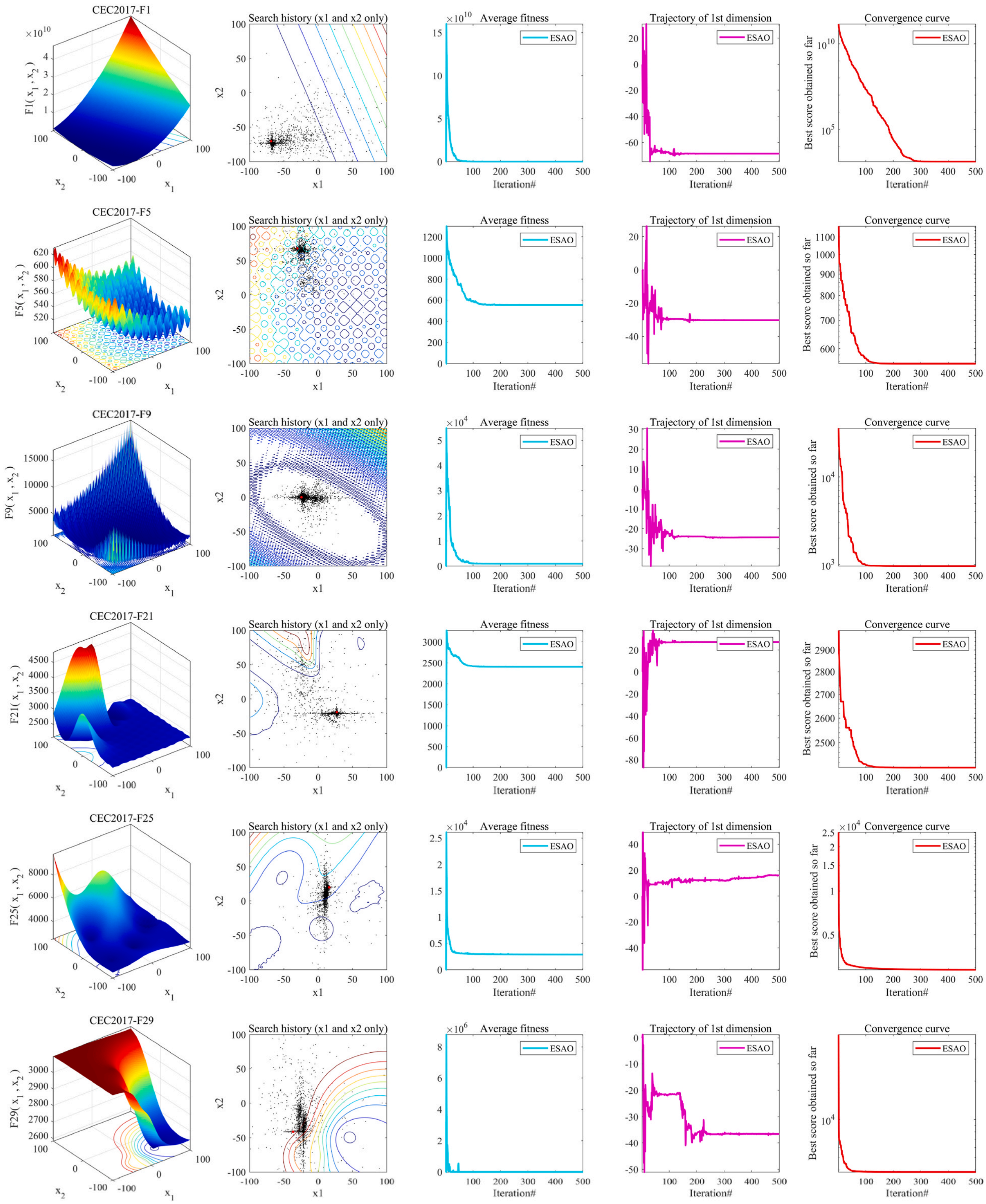

Fig. 3. The convergence behavior of ESAO.

Table 5
Optimization results of CEC2017 from different competitors (Dim = 30).

ID	Metric	WOA	SSA	GJO	COA	PPSO	DECMSA	MELGWO	SAO	ESAO
CEC2017-F1	Avg	5.2941E+09	3.6165E+03	1.1998E+10	1.4559E+09	3.3802E+07	9.6779E+06	1.8966E+09	2.6982E+04	**3.4378E+03**
	Std	1.9313E+09	4.9615E+03	3.6403E+09	2.1527E+09	1.7362E+07	1.6477E+06	2.1594E+09	2.9657E+04	**3.6244E+03**
CEC2017-F3	Avg	2.4600E+05	7.3420E+04	5.9974E+04	1.0575E+05	**2.6859E+04**	7.1996E+04	4.5861E+04	1.2643E+05	3.9473E+04
	Std	7.9490E+04	3.3440E+04	1.1026E+04	2.3448E+04	1.1758E+04	2.9836E+04	**8.6260E+03**	3.7891E+04	2.0009E+04
CEC2017-F4	Avg	1.3651E+03	5.1949E+02	1.4486E+03	6.0960E+02	5.5944E+02	5.0488E+02	5.8416E+02	5.0041E+02	**4.9259E+02**
	Std	3.3207E+02	2.9533E+01	7.0060E+02	1.2874E+02	4.6646E+01	**1.4240E+01**	7.5525E+01	1.9526E+01	3.1073E+01
CEC2017-F5	Avg	8.7813E+02	6.6977E+02	7.1653E+02	7.4532E+02	7.4401E+02	5.9181E+02	6.8287E+02	**5.8149E+02**	5.8630E+02
	Std	5.7651E+01	4.4615E+01	3.8573E+01	5.5229E+01	3.7889E+01	2.7154E+01	4.0826E+01	3.5155E+01	**2.3717E+01**
CEC2017-F6	Avg	6.8030E+02	6.5274E+02	6.4327E+02	6.5390E+02	6.6169E+02	6.0251E+02	6.4226E+02	**6.0099E+02**	6.0462E+02
	Std	1.2747E+01	9.9576E+00	1.1061E+01	1.1788E+01	5.8506E+00	**4.5716E-01**	1.0926E+01	6.5664E-01	3.5492E+00
CEC2017-F7	Avg	1.3155E+03	9.4897E+02	1.0641E+03	1.2296E+03	1.2185E+03	8.8856E+02	1.0400E+03	9.5669E+02	**8.2720E+02**
	Std	8.7840E+01	6.0934E+01	5.8998E+01	9.5697E+01	7.8339E+01	3.3201E+01	8.5345E+01	**2.0758E+01**	3.4249E+01
CEC2017-F8	Avg	1.0716E+03	9.6004E+02	9.9677E+02	9.7826E+02	9.8864E+02	8.8354E+02	9.2791E+02	8.9698E+02	**8.7907E+02**
	Std	4.8684E+01	4.1028E+01	4.3715E+01	2.7621E+01	3.9812E+01	**2.1093E+01**	2.6141E+01	4.9275E+01	2.1115E+01
CEC2017-F9	Avg	1.2332E+04	5.8517E+03	5.3321E+03	7.6206E+03	5.8699E+03	**9.1673E+02**	3.9195E+03	9.7759E+02	1.3666E+03
	Std	3.9659E+03	1.6405E+03	1.1850E+03	1.5070E+03	1.3121E+03	**6.8352E+00**	9.5841E+02	1.0455E+02	3.3516E+02
CEC2017-F10	Avg	7.6810E+03	5.4780E+03	6.9777E+03	6.0840E+03	5.9104E+03	5.8314E+03	5.2218E+03	4.8267E+03	**4.1689E+03**
	Std	8.6420E+02	6.6216E+02	1.3350E+03	7.8161E+02	7.0620E+02	1.0012E+03	6.5575E+02	1.3593E+03	**5.3027E+02**
CEC2017-F11	Avg	1.0555E+04	1.4028E+03	3.7648E+03	1.6980E+03	1.3501E+03	1.4471E+03	1.5036E+03	1.2489E+03	**1.1743E+03**
	Std	4.4634E+03	9.3555E+01	1.5858E+03	4.5122E+02	7.2881E+01	1.9746E+02	4.5779E+02	6.6860E+01	**4.0513E+01**
CEC2017-F12	Avg	4.4499E+08	3.7963E+07	1.1340E+09	1.3974E+07	1.6519E+07	3.2085E+06	4.1964E+07	1.0896E+06	**9.0378E+05**
	Std	2.9175E+08	3.4933E+07	9.5679E+08	1.3667E+07	1.5146E+07	1.8663E+06	6.0861E+07	9.5393E+05	**5.8874E+05**
CEC2017-F13	Avg	1.3690E+07	1.2226E+05	4.0734E+08	2.5822E+05	2.0680E+05	2.3278E+06	1.2249E+05	1.8501E+04	**1.4987E+04**
	Std	1.1730E+07	9.9616E+04	4.6452E+08	4.9203E+05	8.1291E+05	1.6303E+06	7.4202E+04	1.4374E+04	**1.2004E+04**
CEC2017-F14	Avg	3.0530E+06	1.8670E+05	8.4785E+05	5.4299E+05	**4.8031E+04**	2.5007E+05	1.4029E+05	6.4633E+04	1.3068E+05
	Std	3.5023E+06	2.7841E+05	6.6726E+05	6.3342E+05	9.0348E+04	3.5760E+05	1.7084E+05	**7.6768E+04**	8.1411E+04
CEC2017-F15	Avg	5.5030E+06	7.4868E+04	1.6733E+07	3.8773E+04	1.5079E+04	7.0515E+05	2.5728E+04	5.0720E+03	**3.9871E+03**
	Std	7.1652E+06	6.0731E+04	2.5800E+07	3.9799E+04	2.3361E+04	4.1993E+05	1.8319E+04	5.2000E+03	**2.7295E+03**
CEC2017-F16	Avg	4.4173E+03	2.9829E+03	3.0776E+03	3.0350E+03	3.2182E+03	2.6602E+03	2.9295E+03	**2.4059E+03**	2.6016E+03
	Std	7.3220E+02	3.2197E+02	3.9717E+02	3.9640E+02	3.1875E+02	**1.6907E+02**	3.3543E+02	4.2514E+02	3.1000E+02
CEC2017-F17	Avg	2.7633E+03	2.3797E+03	2.3183E+03	2.3139E+03	2.5949E+03	**2.0338E+03**	2.3751E+03	2.0808E+03	2.2396E+03
	Std	2.3648E+02	2.0749E+02	2.7011E+02	2.1836E+02	2.2934E+02	**1.2328E+02**	2.8833E+02	2.0256E+02	2.2489E+02
CEC2017-F18	Avg	1.4058E+07	3.1921E+06	2.1072E+06	2.1247E+06	**2.6323E+05**	5.3698E+05	1.4409E+06	1.3777E+06	6.4807E+05
	Std	1.8861E+07	4.5817E+06	2.6387E+06	2.0376E+06	**3.8661E+05**	4.8293E+05	1.6273E+06	1.2378E+06	7.5094E+05
CEC2017-F19	Avg	2.3593E+07	5.5405E+06	1.2680E+07	3.5954E+04	2.0617E+04	6.9141E+05	1.0865E+05	6.9729E+03	**5.8830E+03**
	Std	1.9705E+07	3.8014E+06	3.0010E+07	6.5962E+04	4.2964E+04	4.7520E+05	1.8934E+05	4.8085E+03	**4.5259E+03**
CEC2017-F20	Avg	2.9031E+03	2.6315E+03	2.5922E+03	2.7170E+03	2.7712E+03	2.4072E+03	2.6243E+03	**2.3471E+03**	2.4452E+03
	Std	2.0072E+02	1.9988E+02	2.0784E+02	2.4735E+02	2.0486E+02	**1.3373E+02**	2.0653E+02	1.8157E+02	2.1406E+02
CEC2017-F21	Avg	2.6204E+03	2.4653E+03	2.4837E+03	2.4768E+03	2.5562E+03	2.4036E+03	2.4442E+03	2.3810E+03	**2.3720E+03**
	Std	5.1399E+01	4.8289E+01	3.5747E+01	4.4569E+01	5.0902E+01	2.6382E+01	2.7363E+01	4.2173E+01	**1.6470E+01**
CEC2017-F22	Avg	8.4846E+03	5.4505E+03	6.5796E+03	4.6282E+03	5.6162E+03	2.5838E+03	5.6384E+03	3.3854E+03	**2.5304E+03**
	Std	1.6651E+03	2.4715E+03	2.3461E+03	2.3931E+03	2.4550E+03	1.4035E+03	1.7778E+03	1.7544E+03	**8.6915E+02**
CEC2017-F23	Avg	3.1471E+03	2.8044E+03	2.9120E+03	2.8940E+03	3.0776E+03	2.7366E+03	2.8289E+03	**2.7178E+03**	2.7526E+03
	Std	8.6348E+01	5.1598E+01	5.2235E+01	8.9355E+01	1.3611E+02	**1.8304E+01**	4.3174E+01	2.1153E+01	3.0456E+01
CEC2017-F24	Avg	3.2732E+03	2.9528E+03	3.0809E+03	3.0199E+03	3.2626E+03	2.9273E+03	2.9853E+03	**2.8852E+03**	2.9067E+03
	Std	8.0308E+01	4.0845E+01	5.6767E+01	5.9201E+01	1.7316E+02	2.6224E+01	5.3987E+01	**2.1199E+01**	2.9365E+01
CEC2017-F25	Avg	3.2259E+03	2.9528E+03	3.2023E+03	2.9759E+03	2.9696E+03	2.8950E+03	2.9749E+03	**2.8896E+03**	2.8923E+03
	Std	6.3930E+01	3.7977E+01	1.2957E+02	3.7048E+01	3.5627E+01	9.7971E+00	4.8308E+01	**6.2105E+00**	1.2655E+01
CEC2017-F26	Avg	8.2043E+03	5.0613E+03	5.9991E+03	6.0614E+03	7.0685E+03	4.6025E+03	5.8716E+03	4.2826E+03	**4.2184E+03**

(*continued on next page*)

Table 5 (*continued*)

ID	Metric	WOA	SSA	GJO	COA	PPSO	DECMSA	MELGWO	SAO	ESAO
	Std	1.3126E+03	1.0797E+03	5.5383E+02	1.6250E+03	1.5672E+03	**2.6074E+02**	6.6062E+02	4.6324E+02	1.1824E+03
CEC2017-F27	Avg	3.5009E+03	3.2892E+03	3.3695E+03	3.2741E+03	3.3952E+03	3.2276E+03	3.2904E+03	**3.2241E+03**	3.2406E+03
	Std	1.4428E+02	4.5079E+01	7.2366E+01	4.2262E+01	1.2460E+02	**7.6908E+00**	3.5444E+01	1.1548E+01	1.6340E+01
CEC2017-F28	Avg	3.9907E+03	3.3115E+03	3.9349E+03	3.3917E+03	3.3131E+03	3.2366E+03	3.4648E+03	3.2465E+03	**3.2185E+03**
	Std	6.9543E+02	4.4305E+01	3.3324E+02	6.5423E+01	3.5240E+01	1.8858E+01	1.1734E+02	3.6504E+01	**1.4716E+01**
CEC2017-F29	Avg	5.5959E+03	4.4595E+03	4.2834E+03	4.1880E+03	4.6315E+03	**3.6177E+03**	4.5054E+03	3.6962E+03	3.8056E+03
	Std	5.6948E+02	2.8694E+02	2.6810E+02	2.4014E+02	4.1674E+02	**7.7979E+01**	3.4322E+02	1.9855E+02	2.5278E+02
CEC2017-F30	Avg	7.5166E+07	8.8680E+06	4.5232E+07	7.1412E+05	4.9776E+05	4.0927E+05	3.1777E+06	1.0785E+04	**9.3614E+03**
	Std	6.1998E+07	5.6203E+06	3.6616E+07	6.6789E+05	6.6675E+05	2.8896E+05	2.0407E+06	**3.1207E+03**	3.5268E+03

Table 6
CEC2017 optimization results for different competitors (Dim = 50).

ID	Metric	WOA	SSA	GJO	COA	PPSO	DECMSA	MELGWO	SAO	ESAO
CEC2017-F1	Avg	2.1293E+10	2.9090E+07	3.6314E+10	1.2891E+10	1.0028E+09	7.0684E+08	1.3370E+10	1.0386E+08	**5.1550E+04**
	Std	5.2793E+09	3.1934E+07	8.6503E+09	6.9079E+09	3.1147E+08	1.1865E+08	5.5549E+09	7.9369E+07	**5.0499E+04**
CEC2017-F3	Avg	2.9911E+05	2.6107E+05	1.4106E+05	3.1985E+05	**1.1602E+05**	2.0036E+05	1.3219E+05	3.3807E+05	1.3021E+05
	Std	9.0065E+04	7.2712E+04	**1.9561E+04**	6.5678E+04	2.0243E+04	2.8226E+04	1.9969E+04	8.6436E+04	4.0690E+04
CEC2017-F4	Avg	4.6411E+03	7.0899E+02	6.3592E+03	2.1314E+03	8.9537E+02	7.3138E+02	2.2525E+03	6.1365E+02	**5.5762E+02**
	Std	1.3088E+03	5.8134E+01	1.7785E+03	8.5474E+02	1.3804E+02	**3.2290E+01**	9.6905E+02	4.4239E+01	5.0689E+01
CEC2017-F5	Avg	1.0925E+03	8.6697E+02	9.3974E+02	9.0539E+02	9.1089E+02	8.0265E+02	8.3864E+02	8.6979E+02	**6.7873E+02**
	Std	8.0115E+01	8.0237E+01	5.9244E+01	**2.3552E+01**	5.4864E+01	6.1513E+01	5.3756E+01	5.8588E+01	4.5936E+01
CEC2017-F6	Avg	6.9874E+02	6.6739E+02	6.5548E+02	6.6928E+02	6.7066E+02	6.1028E+02	6.6118E+02	**6.0977E+02**	6.0978E+02
	Std	1.2061E+01	9.6082E+00	9.4456E+00	4.3155E+00	6.8568E+00	**1.8962E+00**	4.9960E+00	4.5528E+00	5.3025E+00
CEC2017-F7	Avg	1.9151E+03	1.2998E+03	1.4333E+03	1.7708E+03	1.7174E+03	1.2031E+03	1.4641E+03	1.2652E+03	**9.4839E+02**
	Std	1.2088E+02	1.1934E+02	9.4469E+01	7.1250E+01	1.0271E+02	4.1905E+01	1.1276E+02	5.2742E+01	**4.0132E+01**
CEC2017-F8	Avg	1.4017E+03	1.1987E+03	1.2361E+03	1.2298E+03	1.2233E+03	1.0804E+03	1.1520E+03	1.1978E+03	**9.7436E+02**
	Std	8.2975E+01	7.5819E+01	6.6259E+01	**3.6355E+01**	5.5102E+01	4.7246E+01	5.1001E+01	6.1309E+01	3.8323E+01
CEC2017-F9	Avg	3.8850E+04	1.7447E+04	2.3313E+04	2.8785E+04	1.7487E+04	**2.4295E+03**	1.2930E+04	3.5475E+03	2.5802E+03
	Std	8.6737E+03	3.5415E+03	5.3621E+03	6.3358E+03	2.7860E+03	**4.8411E+02**	3.4199E+03	2.1090E+03	7.9639E+02
CEC2017-F10	Avg	1.3156E+04	8.1742E+03	1.1109E+04	1.3393E+04	9.2830E+03	1.0829E+04	8.5861E+03	1.0445E+04	**6.4914E+03**
	Std	**8.0665E+02**	9.1977E+02	2.1351E+03	1.0807E+03	9.3497E+02	2.0987E+03	8.5692E+02	3.0203E+03	8.6473E+02
CEC2017-F11	Avg	8.4030E+03	3.3227E+03	1.0475E+04	6.0344E+03	2.0045E+03	4.7077E+03	4.4996E+03	2.6833E+03	**1.9804E+03**
	Std	2.2752E+03	8.1949E+02	2.5619E+03	2.1913E+03	**2.5803E+02**	1.8652E+03	1.9391E+03	8.6905E+02	4.2949E+02
CEC2017-F12	Avg	4.3410E+09	2.5567E+08	1.0222E+10	4.5136E+08	2.4238E+08	1.7999E+08	1.2402E+09	1.2115E+07	**3.6968E+06**
	Std	1.5162E+09	1.4113E+08	3.7167E+09	9.1224E+08	2.2960E+08	4.0995E+07	1.4066E+09	6.1256E+06	**2.3266E+06**
CEC2017-F13	Avg	5.5547E+08	1.8055E+05	2.8048E+09	2.4053E+06	2.3478E+05	3.4827E+07	1.7681E+08	9.1516E+03	**7.0691E+03**
	Std	6.6513E+08	1.6115E+05	3.3323E+09	2.5925E+06	1.5342E+05	1.2502E+07	7.3095E+08	6.8374E+03	**6.6886E+03**
CEC2017-F14	Avg	7.9215E+06	1.1776E+06	2.8885E+06	1.4996E+06	3.5179E+05	9.5933E+05	1.0946E+06	**2.0698E+05**	4.9796E+05
	Std	5.9587E+06	1.4872E+06	2.8850E+06	1.4998E+06	4.4590E+05	6.0457E+05	1.2852E+06	**1.8218E+05**	4.4215E+05
CEC2017-F15	Avg	7.9792E+07	8.9505E+04	2.8743E+08	9.8459E+04	2.4389E+04	1.3926E+07	1.9060E+06	**1.2269E+04**	1.2501E+04
	Std	6.5753E+07	6.5457E+04	4.0338E+08	8.0585E+04	1.6779E+04	9.8504E+06	6.1874E+06	7.4175E+03	**6.6135E+03**
CEC2017-F16	Avg	6.4898E+03	4.1700E+03	4.1017E+03	4.2096E+03	4.2856E+03	3.8897E+03	3.8413E+03	3.2264E+03	**3.1686E+03**
	Std	1.0353E+03	4.3065E+02	6.1898E+02	6.9510E+02	5.0495E+02	3.0148E+02	**2.7344E+02**	4.1527E+02	3.8910E+02
CEC2017-F17	Avg	4.6496E+03	3.6935E+03	3.7353E+03	3.7002E+03	3.7859E+03	3.4363E+03	3.5051E+03	3.1271E+03	**2.8374E+03**
	Std	6.8271E+02	3.7165E+02	4.0717E+02	4.0752E+02	4.0885E+02	**2.5231E+02**	4.0107E+02	4.7611E+02	3.6649E+02
CEC2017-F18	Avg	5.2568E+07	5.8820E+06	1.7179E+07	7.3179E+06	**1.6023E+06**	3.7728E+06	4.4430E+06	2.9204E+06	1.9747E+06
	Std	4.0018E+07	4.0048E+06	2.1298E+07	6.3300E+06	2.0416E+06	2.2935E+06	2.8608E+06	1.7688E+06	**1.2552E+06**
CEC2017-F19	Avg	1.7547E+07	9.3390E+06	1.8988E+08	4.1963E+05	3.3813E+05	5.6755E+06	1.4676E+06	**1.6367E+04**	1.8907E+04
	Std	1.5458E+07	8.2831E+06	3.3867E+08	5.7195E+05	4.4076E+05	2.5197E+06	5.2769E+06	**8.6805E+03**	1.0606E+04
CEC2017-F20	Avg	3.9066E+03	3.4116E+03	3.4648E+03	3.8130E+03	3.6448E+03	3.5437E+03	3.1690E+03	2.9590E+03	**2.9011E+03**
	Std	3.5039E+02	3.8199E+02	4.5808E+02	2.5354E+02	3.4480E+02	2.1771E+02	**2.0467E+02**	3.7535E+02	2.8610E+02
CEC2017-F21	Avg	3.1095E+03	2.6615E+03	2.7278E+03	2.7348E+03	2.8236E+03	2.5933E+03	2.6577E+03	2.6392E+03	**2.4523E+03**
	Std	9.8222E+01	6.9980E+01	6.6210E+01	9.8564E+01	8.1623E+01	5.3981E+01	4.7904E+01	8.9137E+01	**3.7946E+01**
CEC2017-F22	Avg	1.4710E+04	1.0152E+04	1.3867E+04	1.4294E+04	1.2063E+04	1.1933E+04	1.0678E+04	1.0584E+04	**6.7875E+03**
	Std	1.0435E+03	1.8445E+03	2.2675E+03	2.4172E+03	1.2133E+03	3.7468E+03	**8.5194E+02**	3.1095E+03	3.0816E+03
CEC2017-F23	Avg	3.8548E+03	3.0768E+03	3.3509E+03	3.2892E+03	3.6685E+03	3.0431E+03	3.1807E+03	2.9453E+03	**2.9279E+03**
	Std	1.4653E+02	7.3752E+01	9.1357E+01	1.2434E+02	1.6921E+02	5.8506E+01	8.4701E+01	5.7026E+01	**5.4041E+01**
CEC2017-F24	Avg	3.9084E+03	3.1868E+03	3.5481E+03	3.4370E+03	3.9933E+03	3.2257E+03	3.2864E+03	3.1833E+03	**3.0893E+03**
	Std	1.7983E+02	6.3592E+01	1.1266E+02	1.3321E+02	3.2378E+02	4.7870E+01	9.1001E+01	1.3050E+02	**4.2905E+01**
CEC2017-F25	Avg	5.1652E+03	3.2108E+03	5.8048E+03	4.0246E+03	3.3448E+03	3.2120E+03	4.0739E+03	**3.0996E+03**	3.1023E+03
	Std	7.0457E+02	7.6880E+01	9.0425E+02	5.2896E+02	1.0554E+02	4.9539E+01	4.8270E+02	3.3973E+01	**2.2892E+01**
CEC2017-F26	Avg	1.5755E+04	7.6100E+03	9.7356E+03	1.2113E+04	1.1166E+04	6.9098E+03	9.9638E+03	5.9334E+03	**5.7773E+03**

(*continued on next page*)

Table 6 (*continued*)

ID	Metric	WOA	SSA	GJO	COA	PPSO	DECMSA	MELGWO	SAO	ESAO
	Std	1.5410E+03	2.3285E+03	8.4815E+02	1.3612E+03	2.3931E+03	**4.6534E+02**	1.1952E+03	7.0096E+02	2.0128E+03
CEC2017-F27	Avg	4.7545E+03	3.7161E+03	4.1809E+03	3.8021E+03	4.0463E+03	3.4948E+03	3.9114E+03	**3.4103E+03**	3.5051E+03
	Std	5.6936E+02	1.4094E+02	1.7548E+02	1.8912E+02	3.5780E+02	**5.8498E+01**	1.8654E+02	8.4801E+01	1.1325E+02
CEC2017-F28	Avg	6.1262E+03	3.5912E+03	6.0570E+03	4.5021E+03	3.8104E+03	3.5378E+03	4.8808E+03	**3.3646E+03**	3.3698E+03
	Std	5.9132E+02	1.5718E+02	6.1190E+02	4.2928E+02	2.1427E+02	7.0459E+01	4.8256E+02	**3.6483E+01**	3.9896E+01
CEC2017-F29	Avg	9.3544E+03	6.0000E+03	6.3267E+03	5.6764E+03	6.4031E+03	4.5072E+03	6.1187E+03	**4.1119E+03**	4.2317E+03
	Std	1.3686E+03	7.3421E+02	5.8551E+02	6.1406E+02	6.5275E+02	3.2018E+02	5.7453E+02	**2.8677E+02**	3.3377E+02
CEC2017-F30	Avg	3.1464E+08	1.7013E+08	6.0428E+08	3.5043E+07	2.9639E+07	4.0541E+07	9.1451E+07	1.1681E+06	**9.7239E+05**
	Std	1.1339E+08	5.3060E+07	6.6457E+08	1.5677E+07	1.8650E+07	2.8466E+07	3.4222E+07	2.7278E+05	**2.1574E+05**

Table 7
CEC2017 optimization results for different competitors (Dim = 100).

ID	Metric	WOA	SSA	GJO	COA	PPSO	DECMSA	MELGWO	SAO	ESAO
CEC2017-F1	Avg	1.0656E+11	1.3336E+10	1.3516E+11	7.2467E+10	2.1789E+10	1.7282E+10	7.5019E+10	9.3690E+09	**8.6520E+08**
	Std	9.6047E+09	3.4413E+09	1.4755E+10	1.3934E+10	4.1577E+09	2.8463E+09	1.3272E+10	2.5548E+09	**1.6056E+09**
CEC2017-F3	Avg	9.1921E+05	6.9187E+05	3.9498E+05	7.2575E+05	**3.4901E+05**	5.5829E+05	5.6655E+05	9.7048E+05	4.5343E+05
	Std	1.0123E+05	1.9961E+05	4.9966E+04	8.1139E+04	**3.6401E+04**	6.5300E+04	1.2764E+05	1.8348E+05	9.1685E+04
CEC2017-F4	Avg	2.1618E+04	2.2268E+03	1.8699E+04	9.0276E+03	3.6089E+03	2.5472E+03	1.0196E+04	1.4755E+03	**9.8383E+02**
	Std	2.9851E+03	5.0127E+02	3.3078E+03	1.9252E+03	5.8838E+02	3.9956E+02	3.6540E+03	2.8110E+02	**1.0690E+02**
CEC2017-F5	Avg	1.9583E+03	1.5302E+03	1.5888E+03	1.5380E+03	1.6185E+03	1.4497E+03	1.4270E+03	1.6202E+03	**9.4820E+02**
	Std	1.3256E+02	7.2751E+01	8.0853E+01	**5.1991E+01**	1.0124E+02	8.2185E+01	7.6039E+01	6.5119E+01	7.3093E+01
CEC2017-F6	Avg	7.1058E+02	6.7715E+02	6.7315E+02	6.7322E+02	6.8082E+02	6.2992E+02	6.7268E+02	6.4010E+02	**6.2297E+02**
	Std	1.2683E+01	4.7473E+00	5.6043E+00	**3.1909E+00**	5.7717E+00	4.6480E+00	4.3292E+00	7.0077E+00	5.1954E+00
CEC2017-F7	Avg	3.7761E+03	2.8402E+03	3.0229E+03	3.3856E+03	3.5026E+03	2.2150E+03	3.0139E+03	2.3489E+03	**1.5119E+03**
	Std	1.6482E+02	3.4179E+02	1.4170E+02	1.6845E+02	1.4681E+02	**7.8417E+01**	1.9765E+02	1.7481E+02	1.6072E+02
CEC2017-F8	Avg	2.3993E+03	1.8841E+03	1.9519E+03	2.0266E+03	2.0816E+03	1.7737E+03	1.8602E+03	1.9294E+03	**1.2765E+03**
	Std	1.0511E+02	1.3908E+02	1.0980E+02	**4.5434E+01**	1.0205E+02	9.6623E+01	7.8159E+01	7.6041E+01	7.5677E+01
CEC2017-F9	Avg	8.1541E+04	4.0880E+04	6.5401E+04	5.1886E+04	4.5835E+04	2.6288E+04	3.3951E+04	3.2962E+04	**1.1793E+04**
	Std	1.9718E+04	5.9622E+03	1.1459E+04	1.2796E+04	5.3573E+03	5.6420E+03	**3.4731E+03**	1.1641E+04	3.8399E+03
CEC2017-F10	Avg	2.9099E+04	1.9160E+04	2.5929E+04	2.4217E+04	2.2704E+04	2.9692E+04	1.9895E+04	3.0125E+04	**1.4104E+04**
	Std	**1.0779E+03**	1.5907E+03	4.6355E+03	2.9992E+03	1.5166E+03	3.5671E+03	1.9413E+03	3.6843E+03	1.3624E+03
CEC2017-F11	Avg	3.2385E+05	1.4078E+05	1.1126E+05	3.3542E+05	6.6900E+04	1.0970E+05	6.5594E+04	2.1270E+05	**4.4574E+04**
	Std	1.2609E+05	3.5600E+04	2.8017E+04	1.0960E+05	2.4936E+04	2.5410E+04	**1.5493E+04**	5.5674E+04	1.6028E+04
CEC2017-F12	Avg	3.0638E+10	1.2480E+09	4.7688E+10	1.3185E+10	2.4592E+09	3.1425E+09	2.4578E+10	5.4427E+08	**6.3381E+07**
	Std	8.2236E+09	5.5517E+08	9.8577E+09	7.3450E+09	7.8674E+08	3.8138E+08	1.1869E+10	2.5768E+08	**2.6876E+07**
CEC2017-F13	Avg	3.0526E+09	1.2260E+06	9.6205E+09	5.2042E+08	1.2533E+07	2.6500E+08	2.7897E+09	6.4284E+04	**7.0484E+03**
	Std	1.0872E+09	6.2530E+06	3.7773E+09	8.3559E+08	5.9295E+06	5.3372E+07	2.6600E+09	4.1998E+04	**4.1833E+03**
CEC2017-F14	Avg	2.0954E+07	9.5259E+06	1.5469E+07	9.8053E+06	3.4359E+06	9.3120E+06	5.9795E+06	2.6260E+06	**1.7288E+06**
	Std	8.6981E+06	6.6702E+06	8.7156E+06	5.3790E+06	1.7569E+06	4.8684E+06	2.4477E+06	2.0441E+06	**7.9075E+05**
CEC2017-F15	Avg	4.5318E+08	9.2419E+04	2.8932E+09	8.9436E+07	1.3728E+06	8.2904E+07	5.6172E+08	7.3684E+03	**3.5137E+03**
	Std	2.5344E+08	3.5992E+04	2.0234E+09	2.9242E+08	5.2650E+06	2.5011E+07	1.0056E+09	4.1945E+03	**2.2617E+03**
CEC2017-F16	Avg	1.6897E+04	7.8934E+03	9.3266E+03	8.8231E+03	9.5582E+03	8.9181E+03	8.2689E+03	7.0768E+03	**5.3408E+03**
	Std	2.1860E+03	7.2311E+02	1.0878E+03	1.3673E+03	1.3141E+03	**5.7235E+02**	7.8256E+02	1.9126E+03	7.9057E+02
CEC2017-F17	Avg	2.4091E+04	6.1581E+03	1.8114E+04	6.9365E+03	6.9954E+03	6.8221E+03	7.8466E+03	6.6500E+03	**4.5548E+03**
	Std	1.8047E+04	7.5078E+02	2.3143E+04	7.3386E+02	8.6865E+02	**3.7682E+02**	2.9630E+03	1.3283E+03	4.0592E+02
CEC2017-F18	Avg	1.9902E+07	9.7866E+06	1.9992E+07	1.3588E+07	**4.3900E+06**	1.1431E+07	7.4436E+06	1.1200E+07	4.4148E+06
	Std	8.4137E+06	5.6653E+06	1.1785E+07	1.0078E+07	2.6928E+06	3.9572E+06	4.8211E+06	6.8621E+06	**2.1706E+06**
CEC2017-F19	Avg	4.4736E+08	2.6424E+07	3.3168E+09	1.7397E+07	1.0599E+07	8.7686E+07	3.5325E+08	9.1763E+03	**4.0934E+03**
	Std	2.4906E+08	1.5631E+07	2.8554E+09	1.4874E+07	1.3370E+07	2.9592E+07	8.9364E+08	9.9453E+03	**2.8368E+03**
CEC2017-F20	Avg	7.1625E+03	5.5216E+03	6.4133E+03	7.2673E+03	5.9340E+03	7.3744E+03	5.5262E+03	6.6574E+03	**4.5889E+03**
	Std	5.6620E+02	6.8949E+02	9.6306E+02	4.4250E+02	5.8021E+02	**3.4793E+02**	6.2638E+02	1.4381E+03	6.6824E+02
CEC2017-F21	Avg	4.4711E+03	3.4336E+03	3.5833E+03	3.6894E+03	4.0124E+03	3.2782E+03	3.3856E+03	3.4536E+03	**2.8005E+03**
	Std	2.0697E+02	1.7620E+02	1.1903E+02	1.6368E+02	2.2869E+02	9.2125E+01	1.4416E+02	**6.6259E+01**	8.1191E+01
CEC2017-F22	Avg	3.2156E+04	2.1688E+04	2.8612E+04	3.0066E+04	2.5207E+04	3.2014E+04	2.3779E+04	3.0401E+04	**1.6137E+04**
	Std	**1.6020E+03**	1.6464E+03	4.0841E+03	2.5340E+03	1.7717E+03	3.8032E+03	1.8346E+03	4.1850E+03	4.9645E+03
CEC2017-F23	Avg	5.3595E+03	3.8552E+03	4.4752E+03	4.3272E+03	5.2564E+03	3.6189E+03	4.0261E+03	3.5892E+03	**3.3604E+03**
	Std	2.6243E+02	1.6379E+02	1.6317E+02	2.2633E+02	4.5098E+02	**9.1621E+01**	1.8536E+02	9.2603E+01	1.1455E+02
CEC2017-F24	Avg	6.8169E+03	4.5152E+03	6.0484E+03	5.2808E+03	8.8386E+03	4.4127E+03	4.7678E+03	4.2560E+03	**3.8556E+03**
	Std	4.0919E+02	2.6071E+02	3.3228E+02	4.1520E+02	2.1395E+03	**9.6813E+01**	2.6843E+02	1.1069E+02	1.1797E+02
CEC2017-F25	Avg	1.0790E+04	5.0511E+03	1.2439E+04	8.3675E+03	5.6821E+03	5.2893E+03	8.6363E+03	4.6114E+03	**3.6468E+03**
	Std	1.1447E+03	4.4382E+02	1.7263E+03	1.1187E+03	4.3742E+02	3.2976E+02	1.6881E+03	3.2168E+02	**9.2646E+01**
CEC2017-F26	Avg	3.9634E+04	1.9020E+04	2.7700E+04	3.3274E+04	3.2170E+04	1.7049E+04	2.5439E+04	1.6761E+04	**1.4513E+04**

(*continued on next page*)

Table 7 (*continued*)

ID	Metric	WOA	SSA	GJO	COA	PPSO	DECMSA	MELGWO	SAO	ESAO
	Std	3.3889E+03	3.7218E+03	1.9607E+03	3.0465E+03	6.2603E+03	**1.1074E+03**	4.4479E+03	1.2199E+03	3.9341E+03
CEC2017-F27	Avg	6.1854E+03	4.2377E+03	5.6871E+03	4.5822E+03	4.7905E+03	4.0720E+03	4.6420E+03	**3.5401E+03**	3.6262E+03
	Std	7.6959E+02	1.5146E+02	6.2450E+02	4.0459E+02	5.5246E+02	1.1251E+02	3.7239E+02	**8.7249E+01**	9.4789E+01
CEC2017-F28	Avg	1.4348E+04	6.8446E+03	1.5743E+04	1.1288E+04	7.2381E+03	6.7983E+03	1.0433E+04	4.5685E+03	**3.7909E+03**
	Std	1.1591E+03	1.1112E+03	1.8455E+03	1.4467E+03	9.8773E+02	1.0312E+03	1.6403E+03	4.9037E+02	**1.0533E+02**
CEC2017-F29	Avg	2.0206E+04	1.1056E+04	1.9086E+04	1.1588E+04	1.2309E+04	9.7973E+03	1.2534E+04	7.2448E+03	**6.5996E+03**
	Std	3.6958E+03	1.1750E+03	1.0770E+04	2.0923E+03	1.2091E+03	9.1511E+02	1.8482E+03	6.5684E+02	**5.8212E+02**
CEC2017-F30	Avg	2.8212E+09	4.0472E+08	7.7461E+09	8.3218E+08	1.5853E+08	2.5941E+08	1.8568E+09	6.7623E+05	**4.9626E+04**
	Std	7.6887E+08	1.7869E+08	3.7885E+09	1.0819E+09	7.5467E+07	5.7262E+07	1.4284E+09	4.3800E+05	**2.7932E+04**

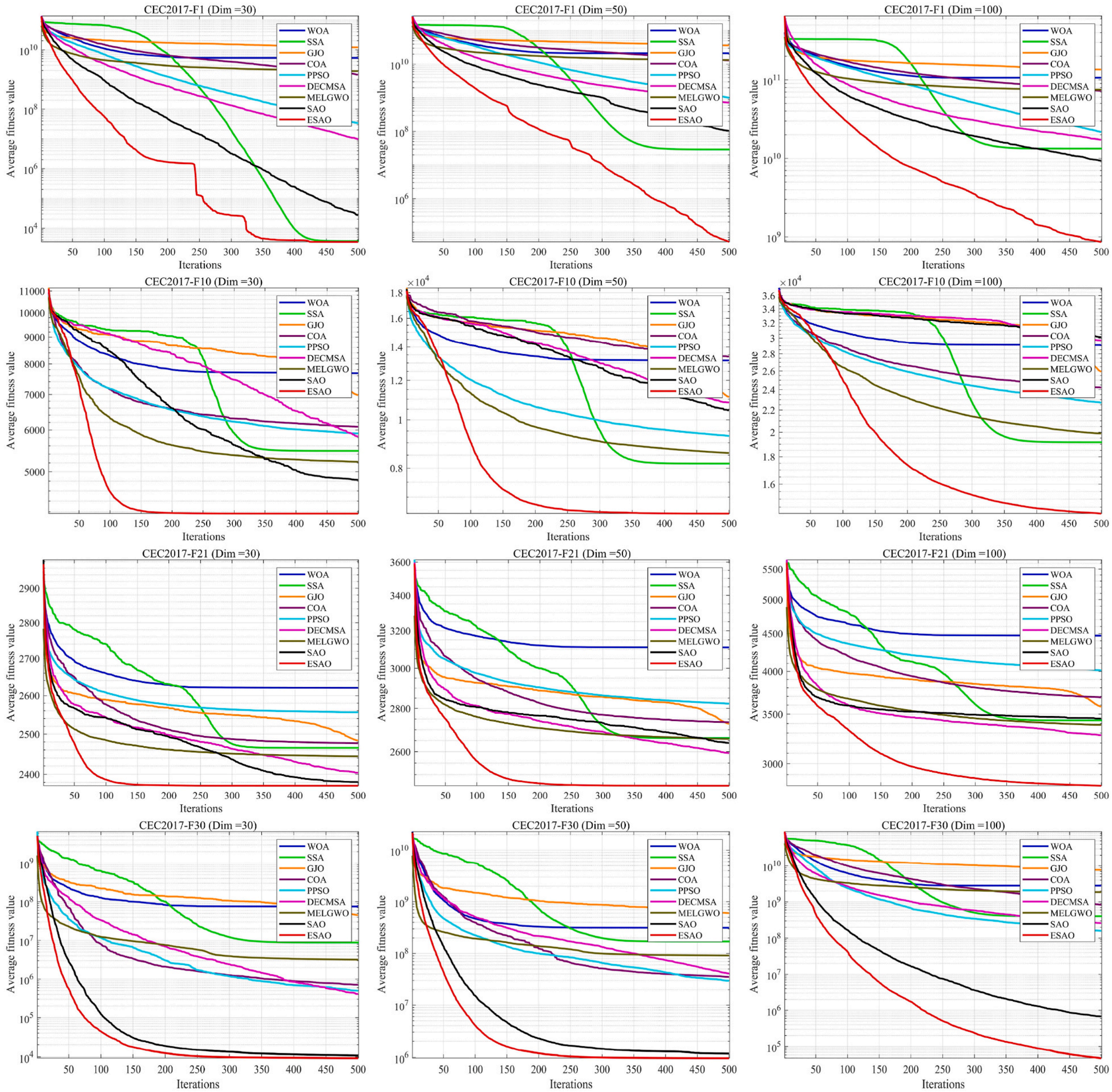

Fig. 4. Comparison of convergence curves of different competitors solving CEC2017.

metric is the path cost J_1, which calculates the total path length of the UAV from the starting point to the endpoint. For each path segment, the total path length is derived by calculating the distance between two adjacent points and summing these distances. This is mathematically expressed by Eq. (16).

$$J_1 = \sum_{i=1}^{N-1} \sqrt{(x_{i+1} - x_i)^2 + (y_{i+1} - y_i)^2 + (z_{i+1} - z_i)^2} \tag{16}$$

where N represents the number of points, (x_i, y_i, z_i) and $(x_{i+1}, y_{i+1}, z_{i+1})$ denote the coordinates of two adjacent points, respectively.

The second metric is the threat cost J_2, which accounts for obstacles or threats along the path by calculating the distance from these threats, thereby increasing the additional cost to encourage the drone to avoid potential dangers. For each path segment, the shortest distance between the segment and each threat is calculated, assigning different cost values based on this distance. This is mathematically expressed by Eq. (18).

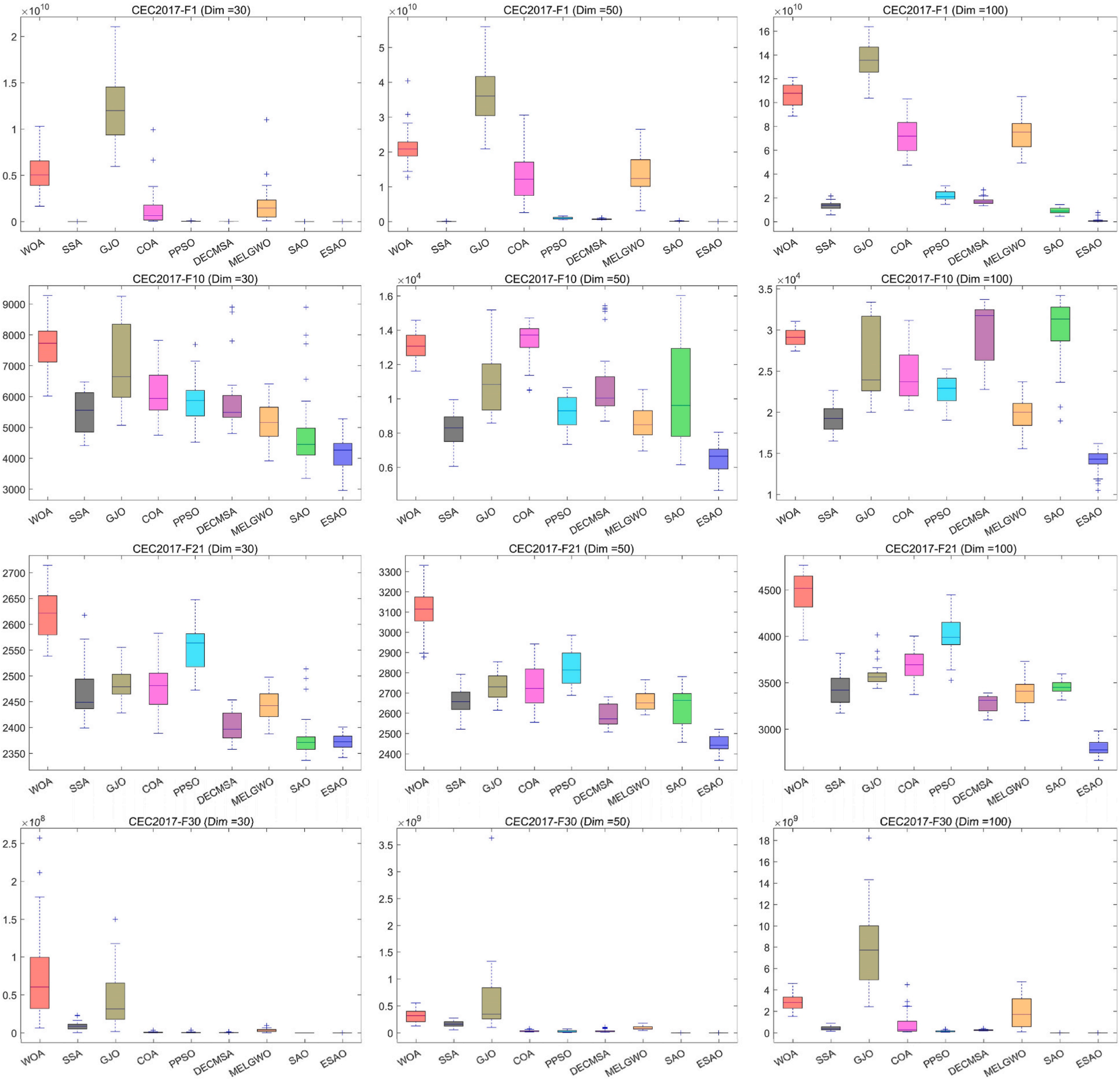

Fig. 5. Comparison of box plots of CEC2017 solved by different competitors.

$$\begin{cases} J'_{2i} = 0, if\ J_r + J_s + J_d > J_{dist} \\ J'_{2i} = 10000000, elseif\ J_r + J_s + J_d < J_{dist} \\ J'_{2i} = J_r + J_s + J_d - J_{dist} \end{cases} \tag{17}$$

$$J_2 = \sum_{i=1}^{N-1} J'_{2i} \tag{18}$$

where J_r, J_s, J_d, and J_{dist} represent the threat radius, UAV size, dangerous distance, and the distance from the UAV to the threat center, respectively.

Then the height cost J_3, considering the height of the UAV flight, it is necessary to avoid hitting the ground and try to keep it in a reasonable height range. For each point on the path, the difference between its height and the ideal height (the intermediate value of h_{min} and h_{max}) is calculated as the cost. The mathematical is denoted in Eq. (20).

Table 8
Comparison with other competitors (Dim = 30).

ID	WOA	SSA	GJO	COA	PPSO	DECMSA	MELGWO	SAO
CEC2017-F1	3.02E-11	**7.06E-01**	3.02E-11	3.02E-11	3.02E-11	3.02E-11	3.02E-11	1.56E-08
CEC2017-F3	3.02E-11	3.02E-11	3.02E-11	3.02E-11	3.02E-11	5.57E-10	3.02E-11	3.02E-11
CEC2017-F4	3.02E-11	2.28E-05	7.20E-05	8.99E-11	6.67E-03	1.25E-05	1.63E-02	5.49E-11
CEC2017-F5	3.02E-11	2.05E-03	3.02E-11	5.07E-10	2.92E-09	**1.30E-01**	2.19E-08	**1.96E-01**
CEC2017-F6	3.02E-11	9.76E-10	3.02E-11	4.98E-11	3.02E-11	**6.41E-01**	1.21E-10	**1.96E-01**
CEC2017-F7	3.02E-11	3.02E-11	3.02E-11	3.02E-11	3.02E-11	**5.37E-02**	3.02E-11	1.49E-06
CEC2017-F8	3.02E-11	4.20E-10	3.02E-11	3.02E-11	3.02E-11	1.60E-07	4.98E-11	3.02E-11
CEC2017-F9	3.02E-11	1.96E-10	3.02E-11	4.50E-11	3.02E-11	**3.95E-01**	1.70E-08	**3.71E-01**
CEC2017-F10	3.02E-11	3.02E-11	3.02E-11	3.02E-11	3.02E-11	3.02E-11	3.02E-11	7.77E-09
CEC2017-F11	3.02E-11	3.50E-09	4.08E-11	6.70E-11	1.21E-10	8.99E-11	1.36E-07	**6.15E-02**
CEC2017-F12	3.02E-11	3.69E-11	3.02E-11	3.02E-11	4.98E-11	3.34E-11	4.08E-11	2.13E-05
CEC2017-F13	3.02E-11	3.02E-11	3.02E-11	8.89E-10	3.02E-11	3.35E-08	3.02E-11	**8.88E-01**
CEC2017-F14	3.02E-11	8.99E-11	3.02E-11	8.15E-11	1.87E-05	3.02E-11	9.92E-11	**3.40E-01**
CEC2017-F15	7.04E-07	**3.95E-01**	3.08E-08	3.37E-04	2.32E-06	**1.26E-01**	**1.30E-01**	3.37E-04
CEC2017-F16	3.02E-11	4.98E-11	3.02E-11	1.21E-10	4.03E-03	3.02E-11	1.09E-10	**5.89E-01**
CEC2017-F17	3.02E-11	4.64E-05	6.28E-06	5.27E-05	2.83E-08	**3.71E-01**	4.98E-04	2.71E-02
CEC2017-F18	5.00E-09	1.12E-02	**3.04E-01**	**1.41E-01**	1.61E-06	1.04E-04	**5.01E-02**	1.63E-02
CEC2017-F19	3.50E-09	1.77E-03	1.37E-03	3.37E-04	2.53E-04	**5.59E-01**	**6.79E-02**	7.96E-03
CEC2017-F20	3.02E-11	3.02E-11	3.02E-11	1.36E-07	3.50E-03	3.02E-11	4.57E-09	**1.62E-01**
CEC2017-F21	5.00E-09	1.52E-03	9.88E-03	6.77E-05	1.49E-06	**6.73E-01**	3.18E-03	**1.41E-01**
CEC2017-F22	3.02E-11	3.34E-11	3.02E-11	5.49E-11	3.02E-11	8.29E-06	4.98E-11	**7.96E-01**
CEC2017-F23	5.49E-11	1.43E-05	2.61E-10	1.17E-09	2.61E-10	7.12E-09	1.46E-10	6.67E-03
CEC2017-F24	3.02E-11	3.16E-05	4.50E-11	3.47E-10	3.02E-11	**7.98E-02**	4.69E-08	7.74E-06
CEC2017-F25	3.02E-11	1.25E-05	3.02E-11	5.07E-10	3.02E-11	1.33E-02	3.08E-08	3.03E-03
CEC2017-F26	3.02E-11	8.10E-10	3.02E-11	6.07E-11	8.99E-11	1.25E-04	5.49E-11	**8.53E-01**
CEC2017-F27	2.61E-10	7.70E-04	3.65E-08	1.09E-05	9.06E-08	**7.73E-01**	1.36E-07	**4.12E-01**
CEC2017-F28	3.02E-11	5.19E-07	3.02E-11	1.89E-04	5.07E-10	1.68E-04	1.70E-08	3.59E-05
CEC2017-F29	3.02E-11	9.92E-11	3.02E-11	3.02E-11	4.08E-11	1.58E-04	3.02E-11	3.77E-04
CEC2017-F30	3.02E-11	2.03E-09	2.03E-07	1.19E-06	8.89E-10	5.26E-04	1.07E-09	**9.05E-02**

Table 9
Comparison with other competitors (Dim = 50).

ID	WOA	SSA	GJO	COA	PPSO	DECMSA	MELGWO	SAO
CEC2017-F1	3.02E-11	3.02E-11	3.02E-11	3.02E-11	3.02E-11	3.02E-11	3.02E-11	3.02E-11
CEC2017-F3	3.02E-11	3.02E-11	3.02E-11	3.02E-11	3.02E-11	3.02E-11	3.02E-11	3.34E-11
CEC2017-F4	2.87E-10	1.29E-09	**7.48E-02**	3.69E-11	**2.90E-01**	5.53E-08	**3.55E-01**	3.69E-11
CEC2017-F5	3.02E-11	2.37E-10	3.02E-11	3.02E-11	3.02E-11	3.02E-11	3.02E-11	9.79E-05
CEC2017-F6	3.02E-11	6.70E-11	3.02E-11	3.02E-11	3.02E-11	5.46E-09	1.09E-10	7.39E-11
CEC2017-F7	3.02E-11	3.02E-11	3.02E-11	3.02E-11	3.02E-11	**2.46E-01**	3.02E-11	**8.88E-01**
CEC2017-F8	3.02E-11	3.02E-11	3.02E-11	3.02E-11	3.02E-11	3.02E-11	3.02E-11	3.02E-11
CEC2017-F9	3.02E-11	3.34E-11	3.02E-11	3.02E-11	3.02E-11	2.37E-10	3.02E-11	4.08E-11
CEC2017-F10	3.02E-11	3.02E-11	3.02E-11	3.02E-11	3.02E-11	**7.06E-01**	3.02E-11	3.15E-02
CEC2017-F11	3.02E-11	5.09E-08	3.02E-11	3.02E-11	6.70E-11	3.02E-11	4.20E-10	1.10E-08
CEC2017-F12	3.02E-11	3.82E-09	3.02E-11	6.70E-11	**6.63E-01**	1.78E-10	9.26E-09	3.77E-04
CEC2017-F13	3.02E-11	3.02E-11	3.02E-11	3.02E-11	3.02E-11	3.02E-11	3.02E-11	5.09E-08
CEC2017-F14	3.02E-11	3.02E-11	3.02E-11	3.02E-11	3.02E-11	3.02E-11	3.02E-11	**1.02E-01**
CEC2017-F15	6.70E-11	**7.73E-02**	3.08E-08	9.79E-05	3.51E-02	1.00E-03	4.21E-02	9.21E-05
CEC2017-F16	3.02E-11	3.02E-11	3.02E-11	7.39E-11	2.53E-04	3.02E-11	7.39E-11	**4.73E-01**
CEC2017-F17	3.02E-11	4.62E-10	2.02E-08	1.07E-07	4.20E-10	4.57E-09	2.39E-08	**4.83E-01**
CEC2017-F18	3.02E-11	1.55E-09	4.62E-10	1.01E-08	2.37E-10	3.96E-08	1.87E-07	**5.01E-02**
CEC2017-F19	8.89E-10	4.42E-06	9.83E-08	1.75E-05	1.63E-02	7.70E-04	1.04E-04	2.42E-02
CEC2017-F20	3.02E-11	3.02E-11	3.02E-11	8.15E-11	6.01E-08	3.02E-11	3.02E-11	**3.87E-01**
CEC2017-F21	1.09E-10	1.03E-06	4.74E-06	8.15E-11	8.10E-10	2.15E-10	4.71E-04	**6.00E-01**
CEC2017-F22	3.02E-11	3.02E-11	3.02E-11	3.02E-11	3.02E-11	4.08E-11	3.02E-11	4.62E-10
CEC2017-F23	3.02E-11	9.83E-08	3.34E-11	2.37E-10	4.50E-11	1.49E-06	1.55E-09	3.37E-05
CEC2017-F24	3.02E-11	1.69E-09	3.02E-11	3.69E-11	3.02E-11	4.57E-09	6.70E-11	**1.62E-01**
CEC2017-F25	3.02E-11	4.69E-08	3.02E-11	3.02E-11	3.02E-11	1.46E-10	9.92E-11	2.71E-02
CEC2017-F26	3.02E-11	2.03E-09	3.02E-11	3.02E-11	3.02E-11	6.70E-11	3.02E-11	**4.29E-01**
CEC2017-F27	3.02E-11	8.12E-04	2.37E-10	4.08E-11	6.52E-09	3.51E-02	2.15E-10	**8.77E-01**
CEC2017-F28	3.02E-11	3.52E-07	3.34E-11	2.83E-08	7.39E-11	**9.00E-01**	1.78E-10	1.06E-03
CEC2017-F29	3.02E-11	7.38E-10	3.02E-11	3.02E-11	3.02E-11	1.21E-10	3.02E-11	**6.10E-01**
CEC2017-F30	3.02E-11	4.08E-11	3.02E-11	6.70E-11	3.02E-11	2.50E-03	3.02E-11	**1.62E-01**

Table 10
Comparison with other competitors (Dim = 100).

ID	WOA	SSA	GJO	COA	PPSO	DECMSA	MELGWO	SAO
CEC2017-F1	3.02E-11	3.69E-11	3.02E-11	3.02E-11	3.02E-11	3.02E-11	3.02E-11	7.39E-11
CEC2017-F3	3.02E-11	3.02E-11	3.02E-11	3.02E-11	3.02E-11	3.02E-11	3.02E-11	3.02E-11
CEC2017-F4	3.02E-11	1.61E-06	7.96E-03	1.78E-10	1.61E-06	5.46E-06	3.18E-04	4.08E-11
CEC2017-F5	3.02E-11	3.02E-11	3.02E-11	3.02E-11	3.02E-11	3.02E-11	3.02E-11	4.20E-10
CEC2017-F6	3.02E-11	3.02E-11	3.02E-11	3.02E-11	3.02E-11	3.02E-11	3.02E-11	3.02E-11
CEC2017-F7	3.02E-11	3.02E-11	3.02E-11	3.02E-11	3.02E-11	4.12E-06	3.02E-11	1.46E-10
CEC2017-F8	3.02E-11	3.02E-11	3.02E-11	3.02E-11	3.02E-11	3.02E-11	3.02E-11	3.02E-11
CEC2017-F9	3.02E-11	3.02E-11	3.02E-11	3.02E-11	3.02E-11	3.02E-11	3.02E-11	3.02E-11
CEC2017-F10	3.02E-11	3.02E-11	3.02E-11	3.02E-11	3.02E-11	6.07E-11	3.02E-11	9.92E-11
CEC2017-F11	3.02E-11	3.02E-11	3.02E-11	3.02E-11	3.02E-11	3.02E-11	4.08E-11	3.02E-11
CEC2017-F12	3.02E-11	4.08E-11	1.21E-10	3.02E-11	6.77E-05	9.92E-11	2.68E-06	3.02E-11
CEC2017-F13	3.02E-11	3.02E-11	3.02E-11	3.02E-11	3.02E-11	3.02E-11	3.02E-11	3.02E-11
CEC2017-F14	3.02E-11	3.02E-11	3.02E-11	3.02E-11	3.02E-11	3.02E-11	3.02E-11	3.02E-11
CEC2017-F15	3.02E-11	1.96E-10	3.02E-11	5.49E-11	1.34E-05	4.08E-11	1.33E-10	**6.15E-02**
CEC2017-F16	3.02E-11	3.02E-11	3.02E-11	3.02E-11	3.02E-11	3.02E-11	3.02E-11	1.19E-06
CEC2017-F17	3.02E-11	6.70E-11	3.02E-11	4.98E-11	3.02E-11	3.02E-11	4.50E-11	1.25E-05
CEC2017-F18	3.02E-11	4.20E-10	3.02E-11	3.02E-11	3.02E-11	3.02E-11	4.08E-11	8.10E-10
CEC2017-F19	2.37E-10	8.29E-06	9.92E-11	3.57E-06	**7.62E-01**	2.67E-09	9.03E-04	2.83E-08
CEC2017-F20	3.02E-11	3.02E-11	3.02E-11	3.02E-11	3.02E-11	3.02E-11	3.02E-11	6.91E-04
CEC2017-F21	9.92E-11	4.80E-07	4.20E-10	6.70E-11	2.03E-09	4.50E-11	2.57E-07	5.09E-08
CEC2017-F22	3.02E-11	3.02E-11	3.02E-11	3.02E-11	3.02E-11	3.02E-11	3.02E-11	3.02E-11
CEC2017-F23	3.02E-11	8.10E-10	3.02E-11	3.02E-11	3.02E-11	3.02E-11	3.02E-11	4.50E-11
CEC2017-F24	3.02E-11	4.50E-11	3.02E-11	3.02E-11	3.02E-11	8.10E-10	3.02E-11	7.12E-09
CEC2017-F25	3.02E-11	4.08E-11	3.02E-11	3.02E-11	3.02E-11	3.34E-11	3.02E-11	1.09E-10
CEC2017-F26	3.02E-11	3.02E-11	3.02E-11	3.02E-11	3.02E-11	3.02E-11	3.02E-11	3.02E-11
CEC2017-F27	3.02E-11	1.41E-04	3.02E-11	3.02E-11	3.02E-11	6.10E-03	3.16E-10	1.56E-02
CEC2017-F28	3.02E-11	3.02E-11	3.02E-11	3.02E-11	3.02E-11	3.02E-11	3.02E-11	4.98E-04
CEC2017-F29	3.02E-11	3.02E-11	3.02E-11	3.02E-11	3.02E-11	3.02E-11	3.02E-11	3.69E-11
CEC2017-F30	3.02E-11	3.02E-11	3.02E-11	3.02E-11	3.02E-11	3.02E-11	3.02E-11	2.84E-04

Table 11
Friedman mean rank test.

Suites	CEC 2017					
Dimension	30		50		100	
Algorithms	Avg. rank	Overall Rank	Avg. rank	Overall Rank	Avg. rank	Overall Rank
WOA	8.90	9	8.60	9	8.50	9
SSA	4.90	4	4.43	4	3.90	3
GJO	6.97	8	7.30	8	7.13	8
COA	6.07	7	6.37	7	5.97	7
PPSO	5.70	6	5.40	6	5.40	6
DECMSA	3.20	3	3.90	3	4.43	4
MELGWO	5.17	5	4.90	5	5.00	5
SAO	2.20	2	2.60	2	3.53	2
ESAO	**1.90**	**1**	**1.50**	**1**	**1.13**	**1**

$$J_3 = \begin{cases} \dfrac{h_i - h_{min}}{h_{max} - h_{min}}, & h_{min} < h_i < h_{max} \\ 10000000, \text{others} \end{cases} \tag{19}$$

$$J_3 = \sum_{i=1}^{N} J_{3i} \tag{20}$$

Finally, the smoothing cost J_4. In order to ensure the smoothness of the flight path, we mainly focus on two aspects: steering angle and climbing angle. The goal here is to ensure that the UAV 's steering and climbing movements during flight are as smooth as possible to avoid the risks and instability caused by sharp steering and climbing. The steering angle and climbing angle between two-line segments formed by three consecutive points on the path are calculated. If these angles exceed the set maximum allowable value, the cost is increased. This is to avoid overly sharp turns or climbs and to ensure the stability of the flight. The mathematical expression is denoted in Eq. (21).

$$J_4 = J_{41} + J_{42} \tag{21}$$

Table 12
Obstacle details.

Index	1	2	3	4	5	6	7	8	9	10
Coordinate (x,y)	(150,350)	(350,100)	(400,500)	(400,650)	(550,450)	(700,150)	(750,350)	(800,800)	(920,600)	(920,200)
Radius	60	50	30	30	40	50	70	50	50	50
Altitude	150	150	150	150	150	150	150	150	150	150

where J_{41} and J_{42} represent the cost of turning and climbing respectively.

5.1.2. Parameter settings

Firstly, we need to set the weights of different costs to calculate the total cost of a single UAV, and the mathematical model is reported in Eq. (22).

$$J_a = w_1 \times J_1 + w_2 \times J_2 + w_3 \times J_3 + w_4 \times J_4 \tag{22}$$

where w represents the weight of different costs. According to their importance, in this article, we set $w_1 = 0.3$, $w_2 = 0.3$, $w_3 = 0.2$, and $w_4 = 0.2$.

Then, in this paper, we solve the cooperative path planning of five Uavs. Therefore, the objective function of this paper is presented in Eq. (23).

$$fobj = \sum_{j=1}^{5} J_a^j \tag{23}$$

where $fobj$ represents the total cost of the drone fleet, and the goal is to minimize it.

Finally, according to the obstacle information in Table 12, we used matlab to build the map as shown in Fig. 6, including the mountain model and multiple obstacles of different scales.

In the preceding section, we completed the modeling of the map. Next, we will use the optimization algorithm developed in this paper (ESAO) and other competitor algorithms to perform path planning for a UAV swarm on this model. For different UAVs, we consider the collision cost shown in Eq. (17) to ensure that the collision risk between UAVs is minimized during flight. Subsequently, we will apply the objective function defined by Eq. (23) for optimization. Using this objective function, we can determine the optimal path for each competitor algorithm under preset constraints. Each algorithm will focus on reducing path length, collision risk, and altitude cost according to its optimization strategy to find the best flight path for the UAV swarm. The next section presents a detailed simulation analysis.

5.1.3. Simulation analysis

In this section, we set the flight start point (150, 150, 50) and the flight end point (900,720,50) of the UAV swarm. Similarly, we compare them to WOA, SSA, GJO, COA, PPSO, DECMSA, MELGWO, and SAO. Each algorithm was run 30 times, and we recorded the best solution (Best), median (Median), worst cost (Worst), mean (Avg), standard deviation (Std), Friedman ranking (F-ranking), Wilcoxon rank sum test results (Wilcoxon). The best results are also highlighted. The experimental results are shown in Table 13. Meanwhile, Fig. 7 displays the average convergence curve across 30 runs. Notably, while other algorithms tend to stagnate, ESAO exhibits a consistent downward trend, indicating a higher likelihood of finding satisfactory solutions. The visualization of path optimization for different competing UAV groups is presented in Figs. 8 and 9, where it is evident that our algorithm produces shorter and smoother paths. In summary, ESAO exhibits not only strong numerical optimization capabilities but also excels in addressing practical problems with robust performance.

5.2. Engineering design problems

In this section, we apply ESAO to two classical engineering design problems.

5.2.1. Pressure vessel design problem

The structure of pressure vessel design problem is shown in Fig. 10. This design goal is to minimize the cost while meeting the requirements of use. Four optimization parameters, including container thickness (T_S), head thickness (T_h), inner radius (R), and length of the container barring head (L). Eq. (24) shows its mathematical model.

Consider:	$\overrightarrow{x} = [x_1\ x_2\ x_3\ x_4] = [T_s\ T_h\ R\ L]$,	(24)
Minimize:	$f(\overrightarrow{x}) = 0.6224x_1x_3x_4 + 1.7781x_2x_3^2 + 3.1661x_1^2x_4 + 19.84x_1^2x_3$,	
Subject to:	$g_1(\overrightarrow{x}) = -x_1 + 0.0193x_3 \leqslant 0$,	
	$g_2(\overrightarrow{x}) = -x_3 + 0.00954x_3 \leqslant 0$,	
	$g_3(\overrightarrow{x}) = -\pi x_3^2 x_4 - \frac{4}{3}\pi x_3^3 + 1296000 \leqslant 0$,	
	$g_4(\overrightarrow{x}) = x_4 - 240 \leqslant 0$,	
Parameters range:	$0 \leqslant x_1, x_2 \leqslant 99, 10 \leqslant x_3, x_4 \leqslant 200$.	

It can be seen from the results of Table 14 that the optimal value of ESAO is better than other competitors, and the result is 5912.708053.

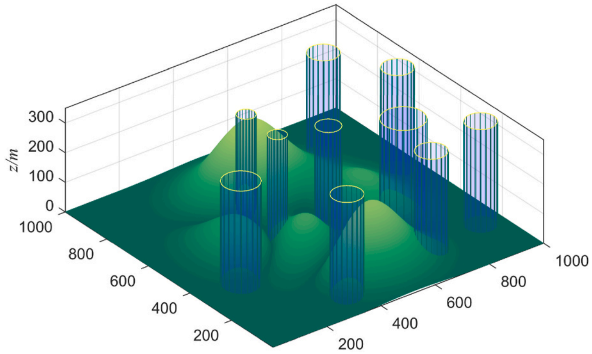

Fig. 6. Map modeling of UAV swarm Path planning.

Table 13
Comparison of UAV swarm path planning optimization results of different competitors.

Algorithms	Best	Median	Worst	Avg	Std	F-ranking	Wilcoxon
WOA	1780.990961	2321.458140	6002170.119763	902188.917834	1604940.235354	9	(+)
SSA	1910.284722	2150.412137	2585.958523	2154.440182	146.289543	7	(+)
GJO	1903.587984	2018.450648	3001892.417280	102007.560774	547700.814744	4	(+)
COA	1834.822565	1996.565092	6002018.946918	202018.071589	1095445.285815	3	(+)
PPSO	1879.926176	2198.686272	3003050.775914	402240.843363	1037406.618726	8	(+)
DECMSA	1907.564298	2016.583192	2309.024872	2042.677168	107.213701	6	(+)
MELGWO	1792.182406	1905.942012	2127.668739	1932.187407	87.336373	2	(+)
SAO	1795.845900	2038.192827	2305.768193	2040.625101	124.616495	5	(+)
ESAO	**1644.057682**	**1713.197327**	**1810.870821**	**1715.386267**	**42.565800**	1	(−)

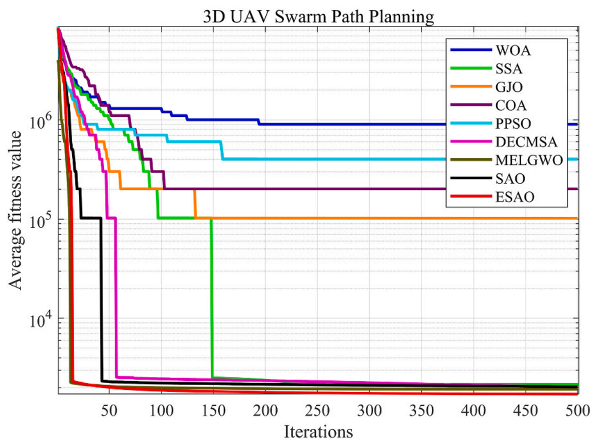

Fig. 7. Comparison of UAVs convergence curves.

5.2.2. *Tension/compression spring design problem*

The design problem is to find three parameters of the spring, including the wire diameter (d), the coil diameter (D), and the number of coils n to minimize the weight of the tension/compression spring. The structure of the engineering problem is shows in Fig. 11, and

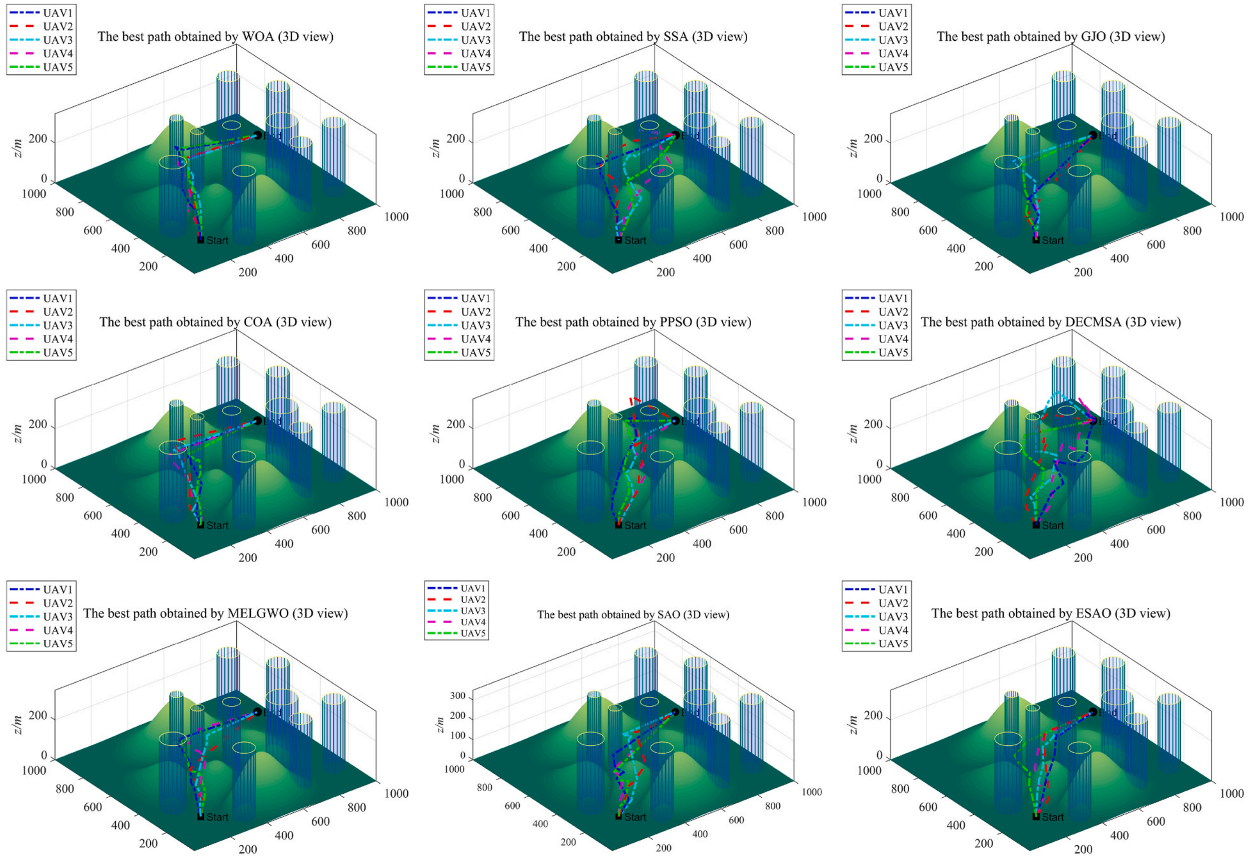

Fig. 8. UAV swarm path optimization results of different algorithms (3D view).

the mathematical model is reported in Eq. (25).

Consider: $$\vec{x} = [x_1 \quad x_2 \quad x_3] = [d\, D\, N], \tag{25}$$

Minimize: $$f(\vec{x}) = (x_3 + 2)x_2x_1^2,$$

Subject to:

$$g_1(\vec{x}) = 1 - \frac{x_2^3x_3}{71785x_1^4} \leqslant 0,$$

$$g_2(\vec{x}) = \frac{4x_2^2 - x_1x_2}{12566(x_2x_1^3 - x_1^4)} + \frac{1}{5108x_1^2} \leqslant 0,$$

$$g_3(\vec{x}) = 1 - \frac{140.45x_1}{x_2^2x_3} \leqslant 0,$$

$$g_4(\vec{x}) = \frac{x_1 + x_2}{1.5} - 1 \leqslant 0$$

Parameters range: $$0.05 \leqslant x_1 \leqslant 2,\ 0.25 \leqslant x_2 \leqslant 1.3,\ 2 \leqslant x_3 \leqslant 1\ 5.$$

5.3. Discussion

Through experimental observation on the CEC2017, UAV swarm path planning, and engineering design problems, we found that the ESAO algorithm generally converges rapidly. However, there is a risk of falling into local optima in some cases, particularly in the later stages of optimization (e.g., CEC2017-F10 and CEC2017-F21). Additionally, when applied to UAV swarm path planning and engineering design problems, ESAO demonstrates superior performance compared to existing state-of-the-art algorithms in terms of convergence accuracy. Nevertheless, when applied in UAV swarm path planning, the convergence rate in the early stages of iteration is slightly lower compared to MELGWO. This is because our proposed strategy enhances the search step size in the early stages of the algorithm.

6. Conclusion

This paper proposes the ESAO technique, designed to address the slow convergence and propensity for becoming trapped in local optima inherent in traditional SAO. ESAO employs a multi-strategy approach, incorporating an adaptive t-distribution control strategy, Cauchy mutation strategy, and leader-based boundary control strategy, to enhance both its global search capabilities and its

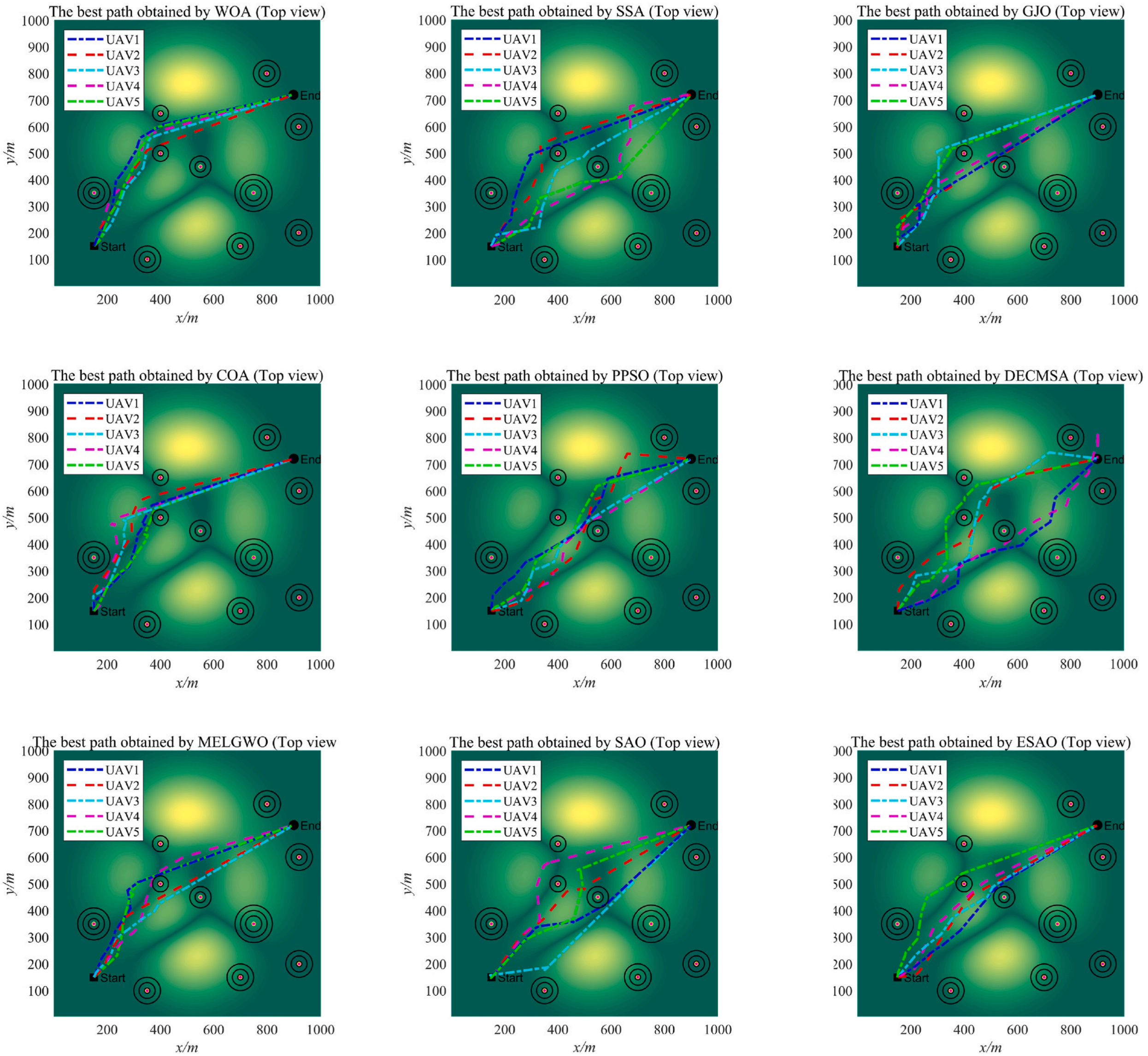

Fig. 9. UAV swarm path optimization results with different algorithms (Top view).

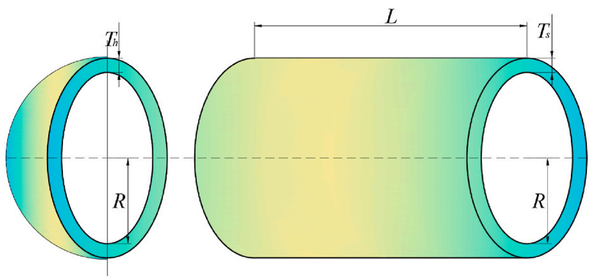

Fig. 10. Schematic representation of the pressure vessel.

Table 14
Comparison results for the pressure vessel design problem.

Algorithm	Optimal values for Parameters				Optimal value
	x_1	x_2	x_3	x_4	
WOA	0.976049	0.755429	48.631552	109.587001	7664.065115
SSA	1.117272	0.552270	57.889681	57.824744	7280.898748
GJO	0.895256	0.447349	46.319551	130.785340	6150.538382
COA	1.104783	0.553671	56.931855	51.376395	6779.366492
PPSO	1.028026	0.508154	53.265593	74.378268	6464.229178
DECMSA	0.861951	0.426064	44.660692	147.277989	6044.519641
MELGWO	0.941754	0.465529	48.795057	108.207080	6228.147368
SAO	0.996497	0.492569	51.631952	85.902903	6373.025441
ESAO	**0.793865**	**0.392408**	**41.132908**	**188.980044**	**5912.708053**

Table 15
Comparison results for the tension/compression spring design problem.

Algorithm	Optimal values for Parameters			Optimal value
	x_1	x_2	x_3	
WOA	0.05634048	0.47928734	6.56952553	0.01303748
SSA	0.05000000	0.31636565	14.16921563	0.01278846
GJO	0.05000000	0.31697006	14.10112896	0.01275894
COA	0.05614531	0.47101427	6.88066122	0.01318580
PPSO	0.05312252	0.39219289	9.47652486	0.01270186
DECMSA	0.05525567	0.44874555	7.40526530	0.01288620
MELGWO	0.05592934	0.46756744	6.87162670	0.01297558
SAO	0.05219230	0.36894553	10.60651493	0.01266981
ESAO	**0.05187177**	**0.36112924**	**11.03494361**	**0.01266584**

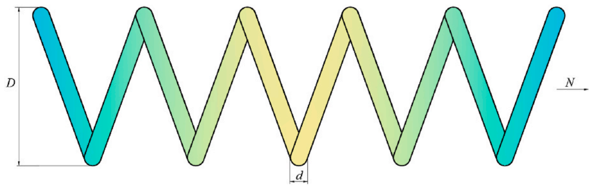

Fig. 11. Schematic representation of the tension/compression spring. The optimization results of different competitors on the tension/compression spring design problem are reported in Table 15. It can be seen that ESAO outperforms other algorithms, and the optimal value is 0.01266584.

ability to escape local optima. Comparative experiments with eight state-of-the-art algorithms on 29 CEC2017 test functions validate ESAO's effectiveness and superiority in global optimization challenges. Furthermore, ESAO has been applied to UAV swarm path planning and engineering design problems, where experimental results demonstrate its superiority over competing algorithms in solution quality and stability, highlighting its potential for practical applications.

Although ESAO demonstrates excellent performance and significantly accelerates the convergence speed of the algorithm, it occasionally falls into local optima. There remain several areas for exploration in future research. We intend to conduct in-depth investigations into ESAO from the following perspectives.

1) Optimizing Parameter Settings: Optimizing ESAO's parameter settings could enhance the algorithm's search efficiency.
2) Exploring Adaptive Mutation and Control Strategies: Investigating additional adaptive mutation and control strategies could further enhance ESAO's global search capabilities and its ability to escape local optima.
3) Application in Practical Problems: Applying ESAO to various practical problems, such as feature extraction, data clustering, parameter identification, and medical diagnosis, could offer a comprehensive evaluation of its performance and applicability.
4) Combining with Other Techniques: Integrating ESAO with other optimization techniques to develop more potent and efficient methods, or creating binary and multi-objective versions, could provide improved solutions for complex real-world problems.

Data availability statement

Data will be made available on request.

CRediT authorship contribution statement

Jinyi Xie: Writing – original draft, Visualization, Supervision, Resources, Conceptualization. **Jiacheng He:** Resources, Methodology, Investigation, Data curation. **Zehua Gao:** Writing – original draft, Validation, Resources, Conceptualization. **Shiya Wang:** Writing – review & editing, Software, Formal analysis, Data curation. **Jingrui Liu:** Writing – original draft, Methodology, Investigation. **Hanwen Fan:** Writing – review & editing, Writing – original draft, Validation, Methodology, Funding acquisition, Data curation.

Declaration of competing interest

The authors declare that they have no known competing financial interests or personal relationships that could have appeared to influence the work reported in this paper.

References

[1] A. Puente-Castro, D. Rivero, E. Pedrosa, A. Pereira, N. Lau, E. Fernandez-Blanco, Q-Learning based system for Path Planning with Unmanned Aerial Vehicles swarms in obstacle environments, Expert Syst. Appl. 235 (2024) 121240.
[2] J. Rabinovitch, R. Lorenz, E. Slimko, K.-S.C. Wang, Scaling sediment mobilization beneath rotorcraft for Titan and Mars, Aeolian Research 48 (2021) 100653.
[3] N. Mohd Noor, A. Abdullah, M. Hashim, Remote sensing UAV/drones and its applications for urban areas: a review, IOP Conf. Ser. Earth Environ. Sci. 169 (2018) 012003.
[4] C. Zhang, W. Zhou, W. Qin, W. Tang, A novel UAV path planning approach: heuristic crossing search and rescue optimization algorithm, Expert Syst. Appl. 215 (2023) 119243.
[5] L. Abualigah, D. Yousri, M. Abd Elaziz, A.A. Ewees, M.A.A. Al-qaness, A.H. Gandomi, Aquila Optimizer: a novel meta-heuristic optimization algorithm, Comput. Ind. Eng. 157 (2021).
[6] S. Kirkpatrick, C.D. Gelatt Jr., M.P. Vecchi, Optimization by simulated annealing, Science 220 (1983) 671–680.
[7] A. Smith, Swarm intelligence: from natural to artificial systems, IEEE Trans. Evol. Comput. 4 (2000) 192–193.
[8] S. Mirjalili, S.M. Mirjalili, A. Lewis, Grey Wolf optimizer, Adv. Eng. Software 69 (2014) 46–61.
[9] T. Bäck, H.-P. Schwefel, An overview of evolutionary algorithms for parameter optimization, Evol. Comput. 1 (1993) 1–23.
[10] J.H. Holland, Genetic algorithms, Sci. Am. 267 (1992) 66–73.
[11] M. Kumar, A.J. Kulkarni, S.C. Satapathy, Socio evolution & learning optimization algorithm: a socio-inspired optimization methodology, Future Generat. Comput. Syst. 81 (2018) 252–272.
[12] S. Fu, H. Huang, C. Ma, J. Wei, Y. Li, Y. Fu, Improved dwarf mongoose optimization algorithm using novel nonlinear control and exploration strategies, Expert Syst. Appl. 233 (2023) 120904.
[13] K. Li, H. Huang, S. Fu, C. Ma, Q. Fan, Y. Zhu, A multi-strategy enhanced northern goshawk optimization algorithm for global optimization and engineering design problems, Comput. Methods Appl. Mech. Eng. 415 (2023) 116199.
[14] D.H. Wolpert, W.G. Macready, No free lunch theorems for optimization, IEEE Trans. Evol. Comput. 1 (1997) 67–82.
[15] L. Deng, S. Liu, Snow ablation optimizer: a novel metaheuristic technique for numerical optimization and engineering design, Expert Syst. Appl. 225 (2023) 120069.
[16] T. Ayyarao, N.S.S. Ramakrishna, R.M. Elavarasan, N. Polumahanthi, M. Rambabu, G. Saini, B. Khan, B. Alatas, War strategy optimization algorithm: a new effective metaheuristic algorithm for global optimization, IEEE Access 10 (2022) 25073–25105.
[17] N. Chopra, M.M. Ansari, Golden jackal optimization: a novel nature-inspired optimizer for engineering applications, Expert Syst. Appl. 198 (2022).
[18] J.K. Xue, B. Shen, Dung beetle optimizer: a new meta-heuristic algorithm for global optimization, J. Supercomput. 79 (2023) 7305–7336.
[19] F.A. Hashim, A.G. Hussien, Snake Optimizer: a novel meta-heuristic optimization algorithm, Knowl. Base Syst. 242 (2022).
[20] H.A. Shehadeh, Chernobyl disaster optimizer (CDO): a novel meta-heuristic method for global optimization, Neural Comput. Appl. 35 (2023) 10733–10749.
[21] Z. Guan, C. Ren, J. Niu, P. Wang, Y. Shang, Great Wall Construction Algorithm: a novel meta-heuristic algorithm for engineer problems, Expert Syst. Appl. 233 (2023) 120905.
[22] M.-Y. Cheng, M.N. Sholeh, Optical microscope algorithm: a new metaheuristic inspired by microscope magnification for solving engineering optimization problems, Knowl. Base Syst. 279 (2023) 110939.
[23] H. Su, D. Zhao, A.A. Heidari, L. Liu, X. Zhang, M. Mafarja, H. Chen, RIME: a physics-based optimization, Neurocomputing 532 (2023) 183–214.
[24] P. Trojovský, M. Dehghani, Subtraction-average-based optimizer: a new swarm-inspired metaheuristic algorithm for solving optimization problems, Biomimetics 8 (2023) 149.
[25] F. Rezaei, H.R. Safavi, M. Abd Elaziz, S. Mirjalili, GMO: geometric mean optimizer for solving engineering problems, Soft Comput. 27 (2023) 10571–10606.
[26] K. Zolfi, Gold rush optimizer: a new population-based metaheuristic algorithm, Operations Research and Decisions (2023) 33.
[27] A.A. Abdelhamid, S.K. Towfek, N. Khodadadi, A.A. Alhussan, D.S. Khafaga, M.M. Eid, A. Ibrahim, Waterwheel plant algorithm: a novel metaheuristic optimization method, Processes 11 (2023) 1502.
[28] N. Fang, Q. Cao, Leaf in wind optimization: a new metaheuristic algorithm for solving optimization problems, IEEE Access 12 (2024) 56291–56308.
[29] W.Y. Zhang, J.A. Zhao, H. Liu, L.P. Tu, Cleaner fish optimization algorithm: a new bio-inspired meta-heuristic optimization algorithm, J. Supercomput. (2024).
[30] R. Sowmya, M. Premkumar, P. Jangir, Newton-Raphson-based optimizer: a new population-based metaheuristic algorithm for continuous optimization problems, Eng. Appl. Artif. Intell. 128 (2024).
[31] S. Fu, K. Li, H. Huang, C. Ma, Q. Fan, Y. Zhu, Red-billed blue magpie optimizer: a novel metaheuristic algorithm for 2D/3D UAV path planning and engineering design problems, Artif. Intell. Rev. 57 (2024) 134.
[32] A.Q. Tian, F.F. Liu, H.X. Lv, Snow Geese Algorithm: a novel migration-inspired meta-heuristic algorithm for constrained engineering optimization problems, Appl. Math. Model. 126 (2024) 327–347.
[33] J. Wang, W.C. Wang, X.X. Hu, L. Qiu, H.F. Zang, Black-winged kite algorithm: a nature-inspired meta-heuristic for solving benchmark functions and engineering problems, Artif. Intell. Rev. (2024) 57.
[34] Y. Fu, D. Liu, J. Chen, L. He, Secretary bird optimization algorithm: a new metaheuristic for solving global optimization problems, Artif. Intell. Rev. 57 (2024) 123.
[35] W. He, X. Qi, L. Liu, A novel hybrid particle swarm optimization for multi-UAV cooperate path planning, Appl. Intell. 51 (2021) 7350–7364.
[36] C. Lu, Y. Lv, Y. Su, L. Liu, UAV swarm Collaborative path planning based on RB-ABC, in: 9th International Forum on Electrical Engineering and Automation (IFEEA), Electr Network, 2022, pp. 627–632.
[37] K. Li, X.X. Yan, Y. Han, Multi-mechanism swarm optimization for multi-UAV task assignment and path planning in transmission line inspection under multi-wind field, Appl. Soft Comput. 150 (2024).
[38] Y. Xiao, H. Cui, A.G. Hussien, F.A. Hashim, MSAO: a multi-strategy boosted snow ablation optimizer for global optimization and real-world engineering applications, Adv. Eng. Inf. 61 (2024) 102464.

[39] H. Jia, F. You, D. Wu, H. Rao, H. Wu, L. Abualigah, Improved snow ablation optimizer with heat transfer and condensation strategy for global optimization problem, Journal of Computational Design and Engineering 10 (2023) 2177–2199.
[40] A.C. Edwards, R. Scalenghe, M. Freppaz, Changes in the seasonal snow cover of alpine regions and its effect on soil processes: a review, Quat. Int. 162–163 (2007) 172–181.
[41] A. Faramarzi, M. Heidarinejad, S. Mirjalili, A.H. Gandomi, Marine predators algorithm: a nature-inspired metaheuristic, Expert Syst. Appl. 152 (2020) 113377.
[42] G. Zhou, M. Cui, J. Wan, S. Zhang, A review on snowmelt models: progress and prospect, Sustainability 13 (2021) 11485.
[43] H.Q. Li, Z.Q. Zheng, Q.G. Lu, Z. Wang, L. Gao, G.C. Wu, L.H. Ji, H.W. Wang, Primal-dual fixed point algorithms based on adapted metric for distributed optimization, IEEE Transact. Neural Networks Learn. Syst. 34 (2023) 2923–2937.
[44] L.L. Liu, D.W. Wang, W.H. Ip, A permutation-based dual genetic algorithm for dynamic optimization problems, Soft Comput. 13 (2009) 725–738.
[45] R. Liu, Y.B. Mo, Y.Y. Lu, Y.C. Lyu, Y.D. Zhang, H.D. Guo, Swarm-intelligence optimization method for dynamic optimization problem, Mathematics 10 (2022).
[46] H. Zhang, Q. Huang, L. Ma, Z. Zhang, Sparrow search algorithm with adaptive t distribution for multi-objective low-carbon multimodal transportation planning problem with fuzzy demand and fuzzy time, Expert Syst. Appl. 238 (2024) 122042.
[47] X. Zhao, Y. Fang, L. Liu, M. Xu, Q. Li, A covariance-based Moth–flame optimization algorithm with Cauchy mutation for solving numerical optimization problems, Appl. Soft Comput. 119 (2022) 108538.
[48] G. Wu, R. Mallipeddi, P. Suganthan, Problem Definitions and Evaluation Criteria for the CEC 2017 Competition and Special Session on Constrained Single Objective Real-Parameter Optimization, 2016.
[49] S. Mirjalili, A. Lewis, The whale optimization algorithm, Adv. Eng. Software 95 (2016) 51–67.
[50] S. Mirjalili, A.H. Gandomi, S.Z. Mirjalili, S. Saremi, H. Faris, S.M. Mirjalili, Salp Swarm Algorithm: a bio-inspired optimizer for engineering design problems, Adv. Eng. Software 114 (2017) 163–191.
[51] H. Jia, H. Rao, C. Wen, S. Mirjalili, Crayfish optimization algorithm, Artif. Intell. Rev. 56 (2023) 1919–1979.
[52] M. Ghasemi, E. Akbari, A. Rahimnejad, S.E. Razavi, S. Ghavidel, L. Li, Phasor particle swarm optimization: a simple and efficient variant of PSO, Soft Comput. 23 (2019) 9701–9718.
[53] X. He, Y. Zhou, Enhancing the performance of differential evolution with covariance matrix self-adaptation, Appl. Soft Comput. 64 (2018) 227–243.
[54] R. Ahmed, G.P. Rangaiah, S. Mahadzir, S. Mirjalili, M.H. Hassan, S. Kamel, Memory, evolutionary operator, and local search based improved Grey Wolf Optimizer with linear population size reduction technique, Knowl. Base Syst. 264 (2023).
[55] F. Wilcoxon, Individual comparisons by ranking methods, Biometrics Bull. 1 (1945) 80–83.
[56] M.H. Nadimi-Shahraki, H. Zamani, DMDE: diversity-maintained multi-trial vector differential evolution algorithm for non-decomposition large-scale global optimization, Expert Syst. Appl. 198 (2022).